Innovative low-cost engineered adsorbents based on eggshell waste for nickel removal from aqueous solutions

Adina-Elena SEGNEANU
Institute for Advanced Environmental Research-West University of Timisoara (ICAM-WUT);
Roxana TRUSCA
National Center for Micro and Nanomaterials, Politehnica University of Bucharest
Claudiu CEPAN
Polytechnic University of Timişoara
Maria MIHAILESCU
Research Institute for Renewable Energy
Cornelia MUNTEAN
University Politehnica Timisoara
Daniel Dumitru HEREA
National Institute of Research and Development for Technical Physics
Ioan GROZESCU
University Politehnica Timisoara, Romania
Athanasios SALIFOGLOU (salif@auth.gr)
Aristotle University of Thessaloniki, School of Chemical Engineering

Article

Keywords: engineered adsorbent, waste reuse, sustainable economy, wastewater remediation, heavy metals, eggshell, zeolite, nickel adsorption

Posted Date: July 20th, 2023

DOI: https://doi.org/10.21203/rs.3.rs-2613416/v3

Additional Declarations: No competing interests reported.

Innovative low-cost engineered adsorbents based on eggshell waste for nickel removal from aqueous solutions

Adina-Elena SEGNEANU[1], Roxana TRUSCA[2], Claudiu CEPAN[3], Maria MIHAILESCU[3,4], Cornelia MUNTEAN[3,4], Daniel Dumitru HEREA[5], Ioan GROZESCU[3] and Athanasios Salifoglou[6,✉]

[1] Institute for Advanced Environmental Research - West University of Timisoara (ICAM-WUT), Str. Oituz, nr. 4, 300086 Timișoara, Romania
[2] National Center for Micro and Nanomaterials, Politehnica University of Bucharest, Str. Splaiul Independenţei, nr. 313, 060042 Bucharest, Romania
[3] University Politehnica Timisoara, Piata Victoriei Nr.2, 300006 Timisoara, Romania
[4] Research Institute for Renewable Energy, 138 Gavril Musicescu St., 300501 Timisoara, Romania
[5] National Institute of Research and Development for Technical Physics, 47 Mangeron Blvd, 700050 Iasi, Romania
[6] Aristotle University of Thessaloniki, School of Chemical Engineering, 54124 Thessaloniki, Greece

1✉ Author to whom correspondence should be addressed

Author E-mail addresses: adina.segneanu@e-uvt.ro; truscaroxana@yahoo.com, cepanclaudiu@gmail.com; mihailescumia@gmail.com; cornelia.muntean@upt.ro; dherea@phys-iasi.ro; ioangrozescu@gmail.com; salif@auth.gr.

Abstract

In contemporary sustainable economy, innovation is prerequisite to waste recycling into new efficient materials, designed to minimize pollution and conserve non-renewable natural resources. Water pollution is a global problem with health, quality of life, and food safety concerns. Thus, waste conversion into cheap, efficient adsorbent materials with high reusability is a challenge in wastewater recycling. In that context, starting from eggshell waste in this study, two new low-cost engineered adsorbents were prepared for the retrieval of nickel from aqueous solutions. Scanning electron microscopy (SEM) results show that, in the first eggshell-zeolite (EZ) adsorbent, the zeolite nanoparticles were loaded in the eggshell pores. The preparation for the second (iron(III) oxide-hydroxide)-eggshell-zeolite (FEZ) adsorbent led to double functionalization of the eggshell base with the zeolite nanoparticles, upon simultaneous loading of the pores of the eggshell and zeolite surface with FeOOH particles. Structural modification of the eggshell led to a significant increase of the specific surface, as confirmed by BET analysis. These features enabled the proposed adsorbents (EZ and FEZ) to remove nickel from aqueous solutions with high performance and adsorption capacities 321.1 mg/g and 287.9 mg/g, respectively. The results indicate that nickel adsorption on EZ and FEZ is a multi-molecular layer, spontaneous, and endothermic process. Concomitantly, desorption results reflect high reusability of these two adsorbents, collectively suggesting the use of waste in the design of new, low-cost, and highly efficient engineered adsorbents for environmental bioremediation.

Keywords: engineered adsorbent, waste reuse, sustainable economy, wastewater remediation, heavy metals, eggshell, zeolite, nickel adsorption.

1. Introduction

Heavy metal removal is a major concern in wastewater treatment, as their concentration is constantly rising due to human activities. In fact, the presence of heavy metals in industrial effluents, as a result of the ongoing intensive global industrialization, is a real danger to human health and the environment, in view of their non-biodegradable nature and incessant accumulation in the human body and soil. Furthermore, climate changes have negatively affected the water cycle, influencing the quality and availability of natural reserves. In this context, it is imperative to adopt a sustainable strategy for water management, the vital source for the existence of life (EPA 2021).

In the industrial world, on the other hand, modern economic growth is directly linked to metal production, prominently pointing toward nickel due to its exceptional physicochemical properties, including high corrosion resistance and toughness, resistance to broad temperature variations, and unique magnetic and electronic properties. In such a context, nickel plays an essential role in the energy industry, transport, pigments, medicine, tannery, food, construction, low-carbon technologies, and batteries for electric cars. However, nickel production and the life cycle of nickel-based materials are associated with a negative environmental impact (El-Naggar 2021; Nakajima 2017; Yokoi 2022). In fact, nickel pollution is a major health hazard. Recent studies report that nickel in contaminated water exhibits high bioavailability, with nickel crossing various biological barriers in the human body (placenta, blood-brain barrier, intestinal), affecting the kidneys, liver, bones, gut microbiota, influencing neurobehavioral functions, the immune system, and causing testicular degeneration, human male infertility, foetal malformations,

systemic contact dermatitis, and cancer (EPSA 2020; Genchi, 2020). According to EU Council Directive 98/83/EC on the quality of water for human consumption, the maximum allowable concentration of nickel in water is 20 μg/L (Council Directive 98/83/EC 1998).

To handle the specific issue, different methods have been reported to remove nickel from wastewater: chemical, electrochemical (electrocoagulation), membrane filtration, adsorption, ion exchange, magnetic field, advanced oxidation, etc. (Qasem, 2021). Each method has advantages and disadvantages related to efficiency, operating costs, and environmental impact. However, adsorption stands out as the most appropriate process for nickel removal due to its simplicity, low operating cost, and high heavy metal removal performance (Öden 2022; Qasem, 2021). In such a process, efficacy depends on the physicochemical properties of the adsorbent, i.e. surface area, porosity, surface reactivity, chemical and thermal stability, selectivity, and regeneration capacity (Fernández-Reyes 2020; Krishna Kumar 2022; Qasem, 2021). Consequently, various adsorbent types (carbon-based, chitosan-based, mineral, magnetic metal-organic frameworks, biosorbents) have been developed over the years and used for heavy metal removal from wastewater (Fernández-Reyes 2020; Krishna Kumar 2022; Qasem, 2021).

In view of the aforementioned grounds, water management in a sustainable economy demands simple, high-performance, eco-friendly, and cost-effective technologies, with a central pillar of this new economic system being the reuse and recovery of waste through innovative materials design of high added value. Implementation of all these ideas, however, requires research creativity riding on specific materials capable of efficiently removing nickel, while concurrently providing for water quality and utilization (European Commission 2015). In such a framework of appropriate materials, zeolites are hydrated aluminosilicates, which belong to the category of mineral adsorbents (Fernández-Reyes 2020; Qasem, 2021), having a series of advantages: they are cheap, ecological, and easily accessible, and most of all they have unique morpho-structural properties (high porosity and resistance to alteration, high ion exchange selectivity, large surface area, and bulk density). Based on such properties, zeolites have been studied in adsorption processes, demonstrating high performance in the removal of various pollutants from wastewater (Al Dwairi, Al-Rawajfeh 2012; Al-Haj, El-Bishtawi 1997; Argun 2008; Fernández-Reyes 2020; Olad 2013; Parades-Aguilar 2021; Rajic 2010; Qasem, 2021)

To this end, current research focuses on the adsorption properties of some materials obtained from agricultural waste of vegetable (vegetable or fruit peel, sawdust, nut shells, fruits seed, tea leaves) or animal (animal bones, crustacean shells, eggshells) origin. The promising literature results open the possibility of developing green and cost-effective methods for sustainable water and waste management (Alquzweeni, Alkizwini 2020; Aman 2008; Annane 2021; Carvalho 2011; El-Azazy 2019; Jai 2007; Waheed 2020). Among such adsorbents, eggshells present a good case of materials. In fact, worldwide, eggshells are produced in vast quantities that end up in landfills, thereby becoming a culture medium for different microorganisms, attracting rodents and other parasites, collectively emerging as a health hazard and an important pollutant according to the Environmental Protection Agency (Mignardi 2020; Waheed 2020). Therefore, re-entry of this waste into an economic cycle to obtain new materials with high added value, including lactose-free dairy products, milk and calcium, biomaterials for orthopaedics and dentistry, animal feed, heavy metal remediation, and fertilizers represents a sustainable solution for both waste and water management (Mignardi 2020; Waheed 2020).

Even if adsorption is the simplest, ecologically sound and cheap method for wastewater remediation, the main shortcomings are dictated by specific adsorbent characteristics, including adsorption rate, selectivity and lifetime. Undoubtedly, clean water is critical for biodiversity, health and life support. Consequently, efficient and inexpensive approaches are required for the development of cheap, eco-friendly adsorbents with high-performance (Chen 2016; Fernández-Reyes 2020; Qasem, 2021; Tripathi, Ranjan 2015).

Although natural adsorbents are a more accessible and cheap option, engineered materials ensure higher adsorption capability (increasing surface area and pore dimension), selectivity and stability (Chen 2016; Fernández-Reyes 2020). In that sense, research on developing engineered waste eggshells through functionalization with α-FeOOH particles reflects substantial improvement in the adsorption capacity of eggshells (Chen 2016; Waheed 2020). In this study, the approach in developing new adsorbent materials moves to a different level, with two different engineered adsorbents from waste eggshells being prepared for immobilizing nickel to be removed from aqueous solutions.

Functionalization of the first adsorbent involves loading the eggshell with zeolite particles. The second adsorbent emerges through simultaneous loading of each component (zeolite and eggshell) with α-FeOOH particles, to ensure considerable increase in sorption sites and surface area for heavy metal ions. Inevitably, each component of the prepared engineered adsorbent is ecological, cheap, and available, with high adsorption capability and cycling stability. To the best of our knowledge, this is the first study reporting on the concurrent use of zeolites and eggshells for efficient removal of nickel from wastewater.

A systematic comparative study of temperature, initial concentration, adsorbent dose, contact time, and pH was also performed to evaluate the influence of experimental conditions on the adsorption capacity of the new adsorbents. The adsorption behavior of both adsorbents was addressed further by conducting adsorption isotherm, kinetic and thermodynamic studies, and adsorption mechanism and desorption kinetics work. The physical and chemical characteristics of this newly engineered adsorbents were studied thoroughly using several analytical methods, including the Brunauer–Emmett–Teller (BET) method, X-ray diffraction (XRD), Fourier-transform infrared (FTIR) spectroscopy, and scanning electron microscopy (SEM). The collective results depict a well-defined profile of newly engineered adsorbents, highly performant, selective, recyclable, low-cost and eco-friendly, and

appropriate for wastewater remediation. Thus, the herein reported study provides a novel, ecological strategy based on waste for efficient nickel recovery from aqueous solutions into new materials with high economic value and environmental performance, exemplified by water remediation and return of nickel to its life cycle, an essential metal in contemporary industry and economy.

2. Methods

2.1. Materials

All used reagents were of analytical grade and purchased from commercial sources (Merck, Alfa Aesar, Sigma-Aldrich). They were used without further purification.

Eggshells (ES) were collected from housework and washed four times with ultrapure water to remove any impurities. Then, they were dried in an oven at 60°C for 3 h. Finally, they were crushed and sieved to obtain a powder of particles with size in the range from 80 to 100 μm (Annane 2021).

Zeolite was bought from Bentonita (Mediesu Aurit, Satu Mare, Romania). It was ground in a mortar and sieved through several ASTM sieves. The present study made use only of particles that passed through a 0.42-mm mesh sift. Zeolite was washed several times with ultrapure water to remove any soluble salts, then dried in an oven for 24 hours at 80°C, cooled down to room temperature, and stored in a desiccator (Al-Haj, El-Bishtawi 1997; Argun 2008). Composite materials comprised of eggshells and zeolite (EZ) as well as iron(III) oxide-hydroxide, eggshells, and zeolite (FEZ) were prepared as stated below (vide infra).

Solutions of Ni(II) (1-30 mg/L) at different concentrations were prepared from a stock solution of $NiCl_2$ (Merck, Darmstadt, Germany), dissolved in an appropriate volume of ultrapure water, subsequently diluting to the desired final concentration(s). For pH adjustment, 1 M HNO_3 or NaOH solutions were used.

2.2. Instrumentation

Phase composition of the derived adsorbents and their components was determined using a Rigaku Ultima IV diffractometer, equipped with a D/teX Ultra detector. The crystallite mean size was calculated through the whole pattern profile fitting method. FT-IR spectra of FEZ and its components in the solid phase were recorded on a Fourier transform infrared spectrometer (Spectrum 100 FT-IR, Perkin–Elmer, Waltham, MA, USA). The surface area of the adsorbent and its components were measured through multi-point regression in the 0.08-0.3 relative pressure range and the (Barrett-Joyner-Halenda) BJH method, respectively, using a Nova 1200e high-speed surface area and porosity analyser (Quantachrome, Boynton Beach, FL, USA). Morpho-structural analysis of the adsorbents was conducted on a SEM-EDS system (QUANTA INSPECT F50), equipped with a field emission gun (FEG). A Jaluba SW23 thermal shaker was used for the batch adsorption experiments. A planetary mill Fritsch Pulverisette was used to prepare the new adsorbents. The initial and residual concentration of heavy metals were determined through an atomic absorption spectrophotometer (Varian SpectrAA 280 FS adsorption, Varian, Palo Alto, CA, USA).

3. Preparation of adsorbents

3.1. EZ adsorbent

To prepare an EZ adsorbent, zeolite and eggshells were mixed in a 1:1 mass ratio. Then, they were mechanically milled, using a planetary mill Fritsch Pulverisette mill 500 rpm for 15 min at 22°C.

3.2. FEZ adsorbent

A 1 M $Fe_2(SO_4)_3$ solution and a 2 M NaOH solution were added dropwise in a flask, under continuous stirring, until the pH of the mixture reached 11.6. The suspension was incubated at room temperature (23°C) for 48 h. Subsequently, FEZ was prepared from EZ and iron(III) oxide-hydroxide (α-FeOOH) (Alfa Aesar) suspension in an EZ:FeOOH = 2:0.25 mass ratio. The resulting mixture was shaken at room temperature for 24 h. Then, it was washed with distilled water several times, filtered, and dried at 70°C for 48 h, thereby affording the engineered adsorbent material.

3.3. Batch adsorption study

The adsorption behavior and mechanism of action for EZ and FEZ were studied by various isothermal, thermodynamic, and kinetics models.

3.3.1. Kinetic study

Kinetic parameters were evaluated to monitor the extent of heavy metal removal. The effect of adsorbent quantity (0.50-3.5 g), contact time (0-460 min), pH (3-9), Ni(II) initial concentration (1-30 mg/L) and temperature (0-50°C) on nickel adsorption kinetics was systematically investigated. Batch tests were conducted in 150 mL Erlenmeyer flasks containing 50 mL of the metal ion solution, with a fixed initial concentration. The flasks were placed on a thermostat shaker at (21.5°C), at 180 rpm steady contact time, with condition variables including pH, adsorbent mass, and temperature of the experiment, until the adsorbate concentration had reached equilibrium. The adsorbent from the emerging suspensions was removed by centrifugation, followed by filtration through Whatman filter paper (0.45 μm). Subsequently, the concentration of nickel in the filtrate was determined by atomic absorption

spectrophotometry. Each experiment was repeated three times. The obtained data and results were accurate to 0.02%.

The amounts of Ni(II) uptake by the adsorbent at equilibrium, Qe (mg/g), were calculated through the following equation (**eq. 1**):

$$Qe = \frac{(C_0 - C_e)V}{M} \text{ (mg Ni/g)} \qquad \textbf{(eq. 1)}$$

Removal efficiency (Re%) was determined as shown (**eq. 2**):

$$\% \text{ Re} = \frac{(C_0 - C_e)\ x\ 100}{C_0} \qquad \textbf{(eq. 2)}$$

where V (mL) represents the volume of solution, M (g) is the weight of the dry adsorbent, C_o and C_e (mg/L) are the liquid phase concentrations of nickel initially and at equilibrium, respectively.

3.3.2. Adsorbent performance

Performance of the prepared adsorbent(s) was evaluated with respect to each one of its components and monitored according to contact time. The employed experimental procedure was the following: Erlenmeyer flasks (150 mL) containing 2.00 g of adsorbent, with a constant volume of nickel solution (50 mL; 25.5 mg/L) at pH 7, were kept at room temperature (22°C) and 200 rpm. During the experiment, samples were collected at different times (0-720 min), centrifuged, and then filtered through Whatman filter paper (0.45 µm). The residual nickel concentration was determined using atomic absorption spectrophotometry (Segneanu 2022).

3.3.3. Desorption study

Experiments were carried out by incubating samples, at room temperature (22°C), containing a constant volume (50 mL) of metal solution (25.5 mg/L) with a fixed amount (2.00 g) of the employed adsorbents in 10 mL of three different solutions (0.1 M HNO_3, 0.1 M HCl or 0.1 M NaOH). The Erlenmeyer flasks were shaken at 200 rpm and test samples were collected every 10 min over the duration of the experiment (0-720 min), centrifuged and then filtered through Whatman filter paper (0.45 µm). The desorbed amount of nickel was determined using atomic absorption spectrophotometry.

The desorption rate was calculated according to the following equation (**eq. 3**):

$$\% \text{ D} = \frac{Cd}{Ca} \text{x}100 \qquad \textbf{(eq. 3)}$$

where,

C_d = amount of metal ion desorbed

C_a = amount of metal ion adsorbed.

To test the FEZ adsorbent reusability, adsorption-desorption cycles were repeated 13 times on the same sample of adsorbent recovered, using a 0.1 M HNO_3 solution (Olad 2013).

The experimental procedure was as follows: To a fixed amount of adsorbent (2.00 g) mixed with a constant volume (50 mL) of nickel solution (25.5 mg/L), 25 mL of HNO_3 (0.1 M) was added. The mixture was shaken at 200 rpm at room temperature (22°C) for 5 h, centrifuged and then filtered (0.45 µm). Nickel residual concentration was determined using atomic absorption spectrophotometry.

3.3.4. Kinetic studies

Experiments were carried out at constant temperature (40°C) and pH value (pH 7), with 2.00 g of absorbent and 50 mL nickel solution (25.5 mg/L). The samples were retrieved at different times (0-360 minutes) (Lyubchik 2016).

3.3.5. Thermodynamic study

Experiments were carried out at three different temperatures (295.15K, 303.15K, and 313.15K) at pH 7, using a fixed amount of adsorbent (2.00 g) and constant volume of nickel stock solution (50 mL; 25.5 mg/L). Adsorption thermodynamic diagrams were generated by plotting lnK (abscissa) vs 1/T (ordinate). The correlation coefficient $R^2 = 0.9996$ (FEZ) and $R^2 = 0.9994$ (EZ) demonstrates good linear relationship of the derived data.

3.3.6. Statistical analysis

Each experimental set was performed in triplicate, using one-way analysis of variance (ANOVA) without replication; $p < 0.05$ is taken as statistically significant.

Results

4.1. BET analysis

Surface properties for FEZ and its component materials (zeolite and eggshell) were examined using low-temperature (77K) nitrogen adsorption-desorption isotherms. Surface areas and pore size distributions were determined using the Brunauer–Emmett–Teller (BET) and Barrett-Joyner-Halenda (BJH) methods. The obtained results are presented in **Table 1**.

Table 1. Parameters of the newly prepared adsorbents and components thereof determined through BET*

Sample	Surface area (m^2/g)	Average pore size diameter (nm)	Total pore volume (cm^3/g)
Eggshell	1.311	8.347	$2.03\ 10^{-3}$
Zeolite	12.111	15.574	$38.06\ 10^{-3}$
EZ	19.321	7.132	$11.20\ 10^{-3}$
FEZ	23.901	4.023	$8.10\ 10^{-3}$

* standard deviation (SD) = 0.02%

According to the data, the eggshell BET/N_2 specific surface is 1.311 m^2/g, a value similar to that reported in the literature (Annane 2021; Tsai 2008). The corresponding value for zeolite is 12.111 m^2/g, analogous to that in the literature (Argun 2008). The textural properties of ZEF are different from its components, i.e. eggshell and zeolite. Thus, the specific surface of FEZ is 23.901 m^2/g.

The isotherms of FEZ (**Figure 1**) fitted a type II isotherm with an H3 hysteresis loop and a type IV isotherm with an H3 hysteresis loop for the EZ adsorbent, zeolite, and eggshell (mesoporous structure) (Thommes 2015).

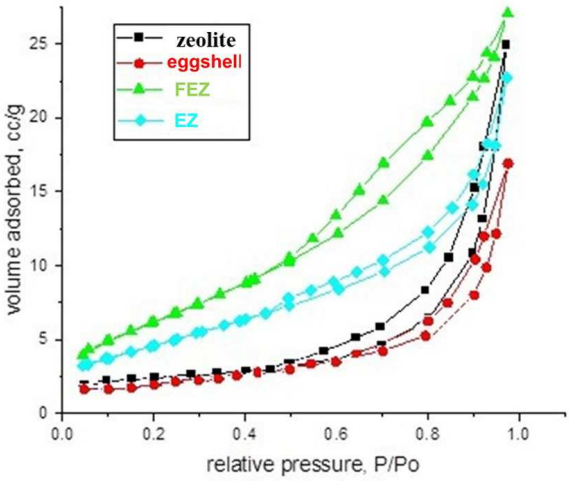

Figure 1. Nitrogen adsorption-desorption isotherms for FEZ adsorbent, EZ, eggshell, and zeolite

4.2. FT-IR spectroscopy

FT-IR spectra were recorded for EZ, FEZ, and their starting material components (zeolite and eggshell) (**Figure 2, 1SA-D**). The spectrum for EZ shows eggshell vibrational bands at ~714 cm^{-1} (Ca-O stretch), 873 and 1423 cm^{-1} (C-O stretch), 1802 and 2519 cm^{-1} (attributed to O-C-O), 1643 cm^{-1} (assigned to N-H), and 2976 cm^{-1} (symmetric and antisymmetric C–H stretching vibrations) (Annane 2021; Chen 2016; Segneanu 2022; Xin 2018). The weak band at ~1387 cm^{-1} is likely due to nitrate impurities from the KBr pellet (Chukanov NV, Chervonnyi 2016).

The peaks associated with the zeolite component are found at 3625 cm^{-1}, attributed to Si-OH-Si or Al-OH-Al, ~1057 and 797 cm^{-1}, corresponding to Si-O stretching vibrations in quartz, 608 cm^{-1} assigned to Si-O-Al and Si-O-Si bending vibrations, and 469 cm^{-1} attributed to Si-O-Si vibrational deformation (Argun 2008; Zendelska 2018).

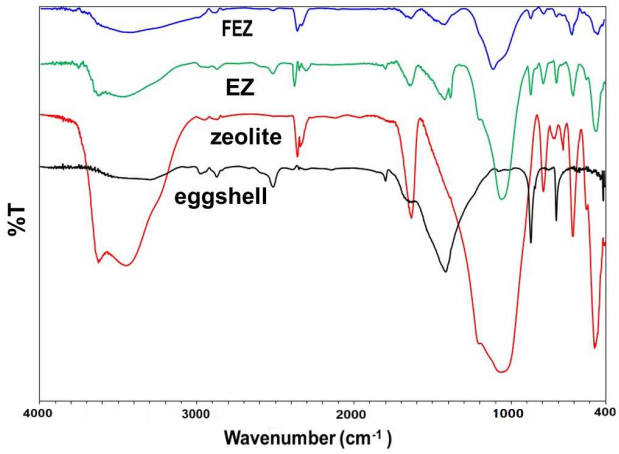

Figure 2. FT-IR spectra of FEZ, EZ, eggshell, and zeolite

The FEZ spectrum exhibits the eggshell characteristic peaks at 714 cm^{-1} (associated with Ca-O stretch), 872 and 1420 cm^{-1} (C-O stretch), 1802 and 2517 cm^{-1} (attributed to O-C-O), 1647 cm^{-1} (assigned to N-H) and 2976 cm^{-1} (symmetric and antisymmetric C–H stretching vibration) (Annane 2021; Chen 2016; Segneanu 2022; Xin 2018). Features associated with the zeolite component are found at 3624 cm^{-1}, attributed to Si-OH-Si or Al-OH-Al, ~1055 and 797 cm^{-1}, corresponding to Si-O stretches in quartz, 608 cm^{-1} attributed to a bending vibration Si-O-Al and Si-O-Si, and 469 cm^{-1} assigned to the Si-O-Si vibrational deformation (Argun 2008; Zendelska 2018).

It appears that the EZ spectrum displays the functional groups of its components (eggshell and zeolite), thus demonstrating the successful preparation of the material. Furthermore, the stretching vibrations of Fe–OH (450, 410 cm^{-1}) and Fe–O (632 cm^{-1}) reflect the presence of α-FeOOH particles on eggshell and zeolite, thus pointing to a successful preparation of FEZ (Kaufhold 2022).

4.3. SEM analysis

The surface morphology, shape, and particle size of both proposed adsorbents (EZ and FEZ), as well as their components (eggshell and zeolite), were studied by SEM (**Figure 3**).

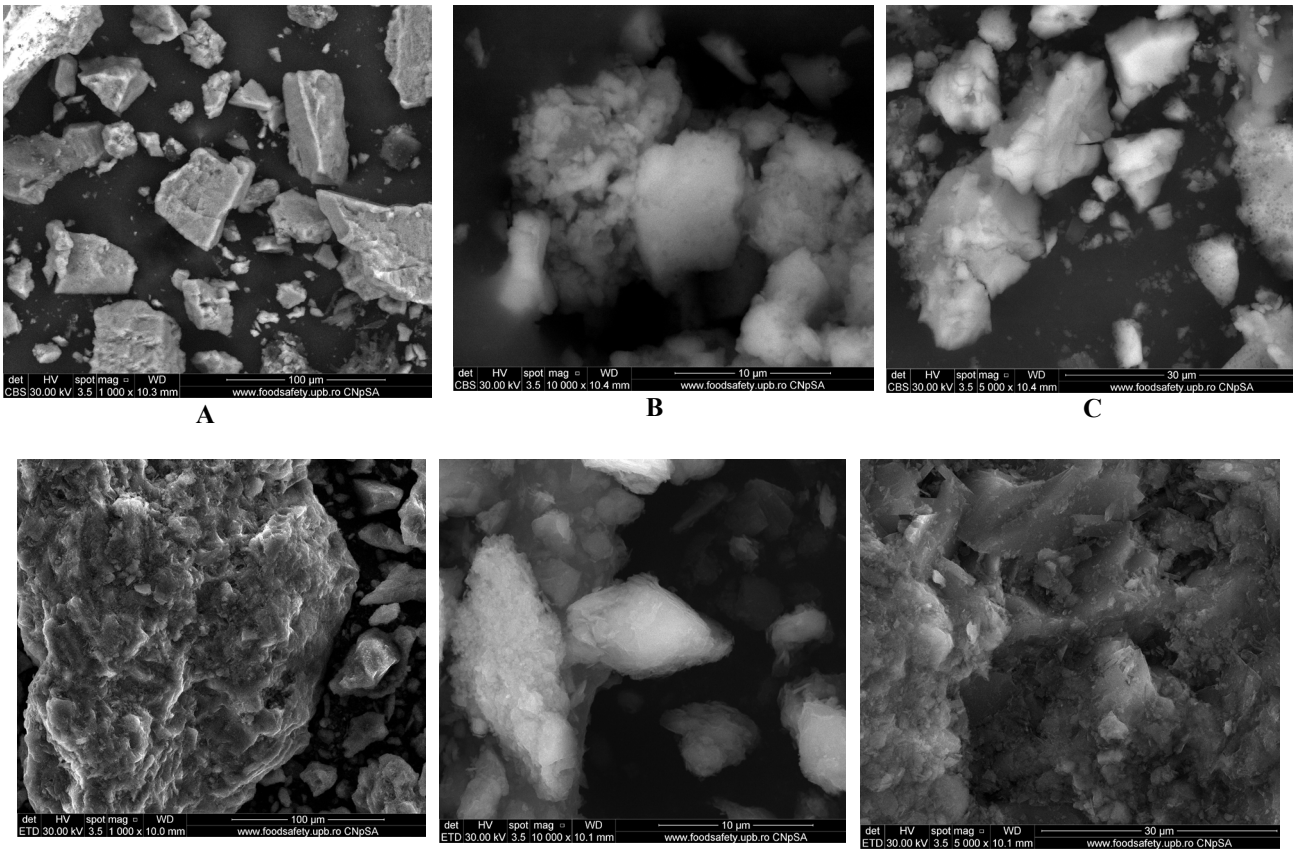

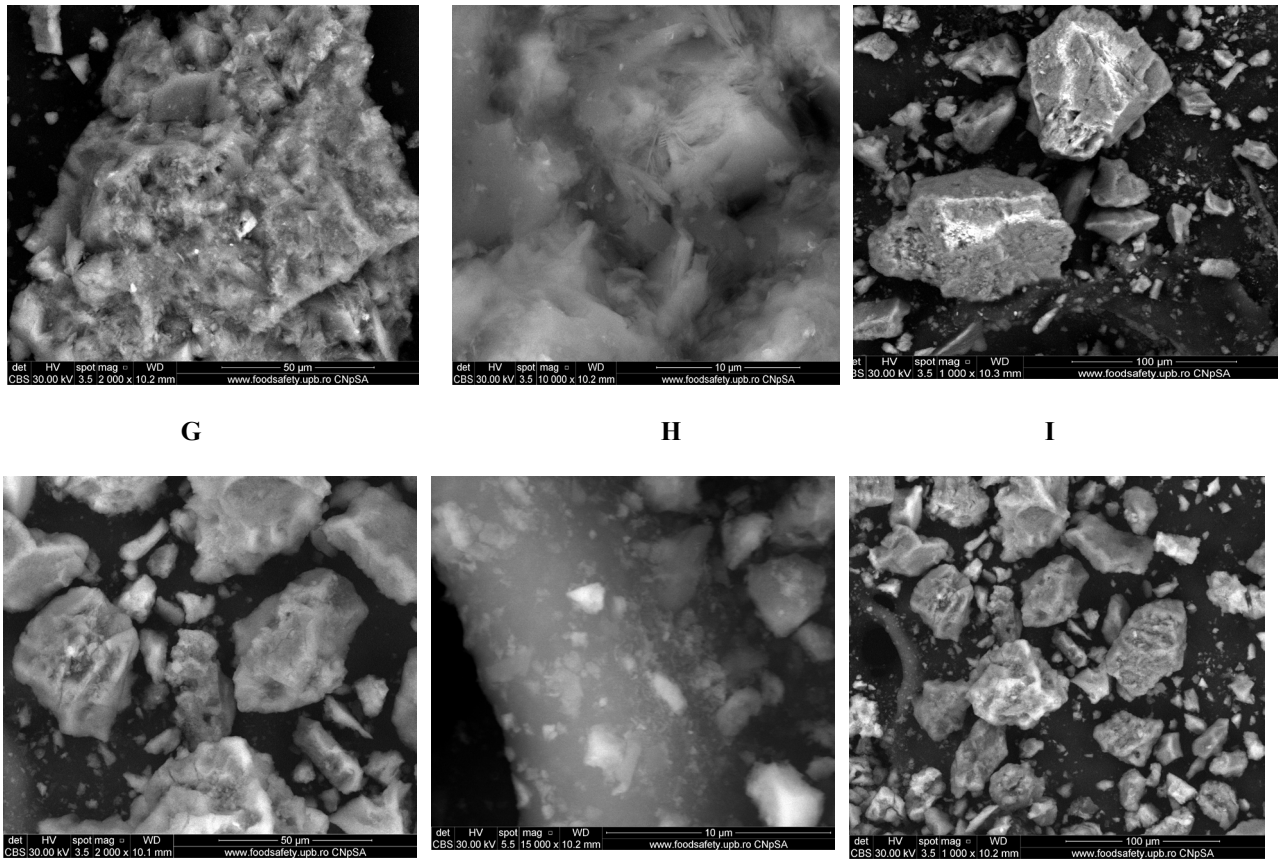

Figure 3. SEM images of eggshell (**A,B,C**), zeolite (**D,E,F**), EZ (**G,H,I**), and FEZ (**J,K,L**) adsorbents

It appears that eggshell micrographs (**Figure 3A-C**) indicate the presence of multiporous and irregular shape agglomerations of different size particles (average size ~80 nm) (Chen 2016; Park 2007). Zeolite micrographs (**Figure 3D-F**) exhibit agglomerations of cubic and rectangular crystals of nanometric dimensions (~20 nm). EZ micrographs (**Figure 3G-I**) indicate the presence of clusters of particles of different sizes in the nano-size regime, cubic, rectangular-shaped crystals, and irregular crystal structures loaded in the pores of eggshell particles. FEZ micrographs (**Figure 3J-L**) show the same clusters of different nano-sized particles (~17.4 nm) as in EZ. Nonetheless, a notable difference appears specifically in the cluster size decrease. Another visible aspect is the presence of numerous uniform nano-size particles (~7 nm), loaded in zeolite and eggshell pores that could be attributed to α-FeOOH particles (Chen 2016).

Accompanying the SEM spectra are EDX analyses on the elemental composition of all samples investigated (**Figure 2S-3S**). The EDX spectra of eggshell samples are in good agreement with data reported in the literature (Mignardi 2020), with zeolite data also corroborating those in the literature (Zendelska 2018). Work on the emerging EZ adsorbent material, using SEM and EDX analysis, indicates the presence of both eggshell and zeolite components in it (**Figure 4**). Analogous work with FEZ shows similar behavior upon introduction of the ternary component of iron (**Figure 3SB**).

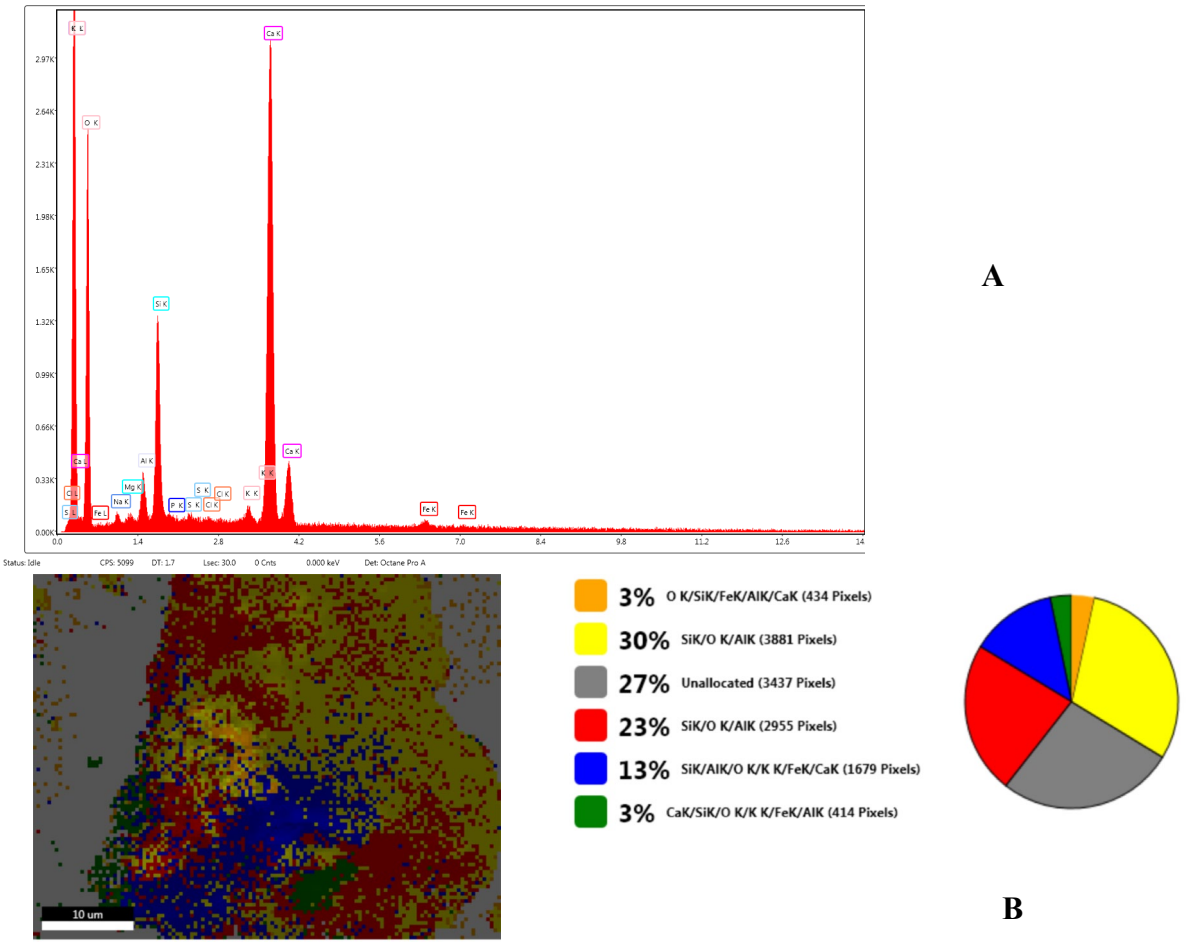

Figure 4. (**A**) EDX composition, and (**B**) SEM-EZ live map for EZ and the distribution of the identified elements

In fact, the EDX spectrum for FEZ (**Figure 3S**) shows that the iron peaks are much more intense than in EZ (**Figure 4**), where iron peaks come only from zeolite (**Figure 1S**). Comparative analysis of live maps for FEZ (**Figure 3SB**) and EZ (**Figure 3SA**) shows the differences in identified element ratio in these two adsorbents due to the functionalization with α-FeOOH.

The collective results suggest that functionalization of EZ with FeOOH led to a new adsorbent material with a unique structure, i.e. double functionalization of eggshell, with the nano-size particles of zeolite achieved simultaneously upon loading of the pores of the eggshell and zeolite surface with α-FeOOH particles. The EZ adsorbent structure modification through functionalization with α-FeOOH led to the active surface increase, an aspect confirmed by BET analysis (**Table 1**). The adsorbent surface enhancement projects a higher amount of sorption sites available, suggesting improvement in adsorption performance. A schematic representation of both adsorbent structures (EZ and FEZ) is presented in the next Figure (**Figure 4.1**)

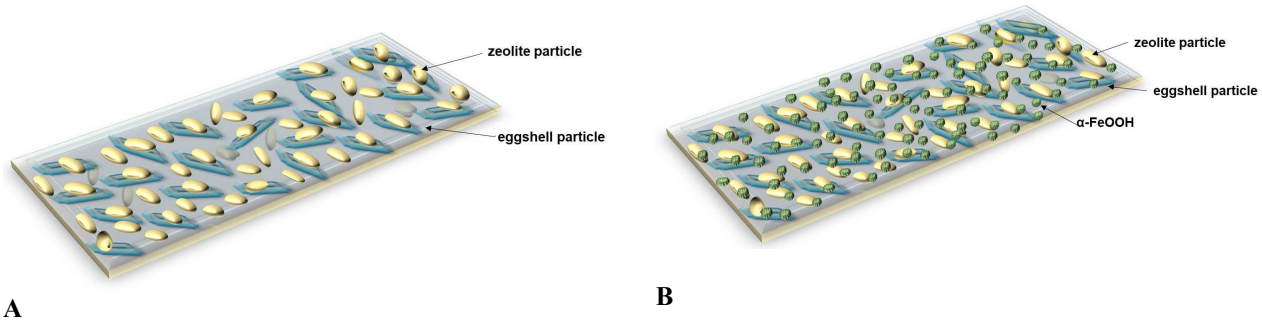

Figure 4.1 Schematic representation of adsorbents structure (**A**) EZ, and (**B**) FEZ

4.4. XRD study

The XRD spectrum of zeolite (**Figure 4SA**) shows the diffraction peaks of the crystalline phase $Al_{6.97}Ba_{0.33}Ca_{1.57}K_{0.57}Mg_{0.72}Na_{1.92}O_{96.41}Si_{29.04}$ (clinoptilolite-Ca) (database card no. 9001509), with a crystallite mean size of 24.7 nm. The corresponding spectrum of eggshell (**Figure 4SB**) shows diffraction peaks of the single crystalline phase of calcite $CaCO_3$ (database card no. 9007689), with a crystallite mean size of 87.2 nm (Annane 2021; Park 2007).

In the XRD spectrum of EZ (**Figure 5** and **4SC**), only two crystalline phases, i.e. calcite $CaCO_3$ from eggshell and $Al_{6.97}Ba_{0.33}Ca_{1.57}K_{0.57}Mg_{0.72}Na_{1.92}O_{96.41}Si_{29.04}$ (clinoptilolite-Ca) from zeolite, are visible. This result confirms the nature of the EZ absorbent. The XRD spectrum of FEZ (**Figure 5** and **4SD**) shows only two crystalline phases: clinoptilolite-Ca ($Al_{6.97}Ba_{0.33}Ca_{1.57}K_{0.57}Mg_{0.72}Na_{1.92}O_{96.41}Si_{29.04}$ (database card no. 9001509) and calcite ($CaCO_3$, database card no. 9007689). Although according to the synthesis procedure and EDX results (**Figure 3SB**), iron is in large proportion in the material (mass ratio EZ:FeOOH = 2:0.25) and therefore it should be in the form of α-FeOOH, iron does not appear in the spectrum. That is likely due to the amorphous form of α-FeOOH, as a result of which it does not appear in the XRD spectrum of FEZ. The FEZ material was calcined at 300°C and 700°C to transform α-FeOOH from the amorphous to the crystalline Fe_2O_3 phase, in order to demonstrate the presence of α-FeOOH and implicitly validate the FEZ preparation. After heating the material at 300°C, the spectrum shape remained identical, showing the same crystalline phases as prior to heating.

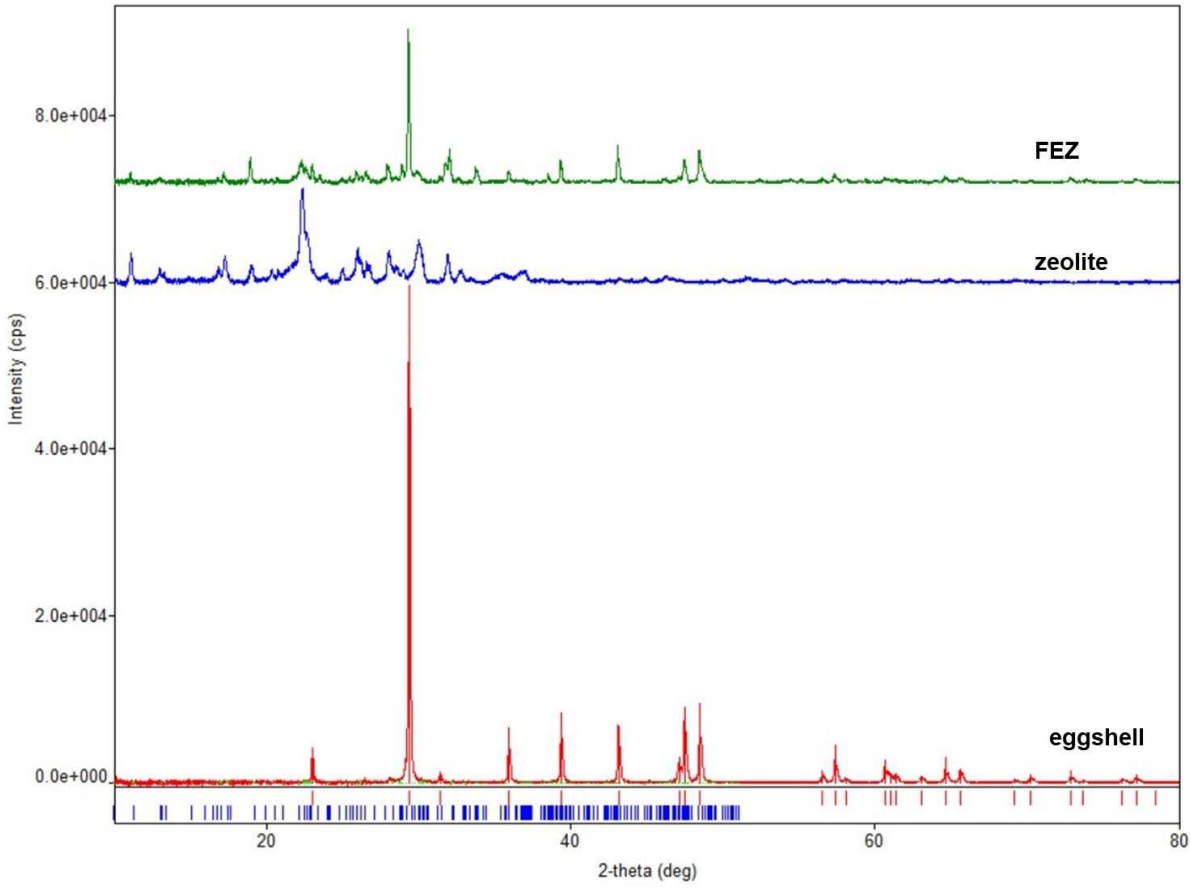

Figure 5. XRD spectra of eggshell, zeolite, EZ, and FEZ

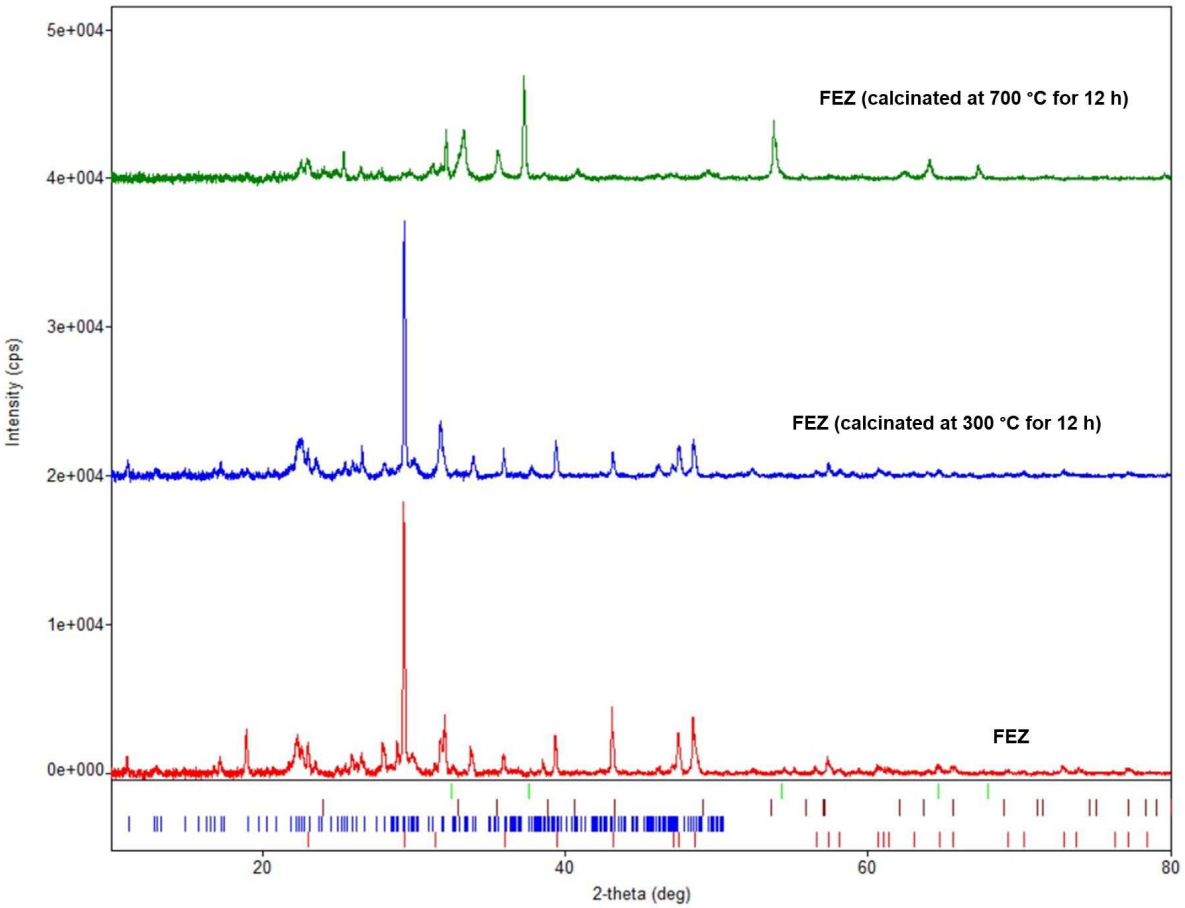

Figure 6. XRD spectra of ZEF before and after calcination at 300°C and 700°C

The spectrum of the material heated at 700°C (**Figure 6**) is entirely different. The diffraction peaks of clinoptilolite-Ca are considerably smaller. Only the most intense ones are still visible. The calcite peaks disappeared due to $CaCO_3$ decomposition (red lines under the XRD peaks; **Figure 6**) to CaO and CO_2, as proven by the presence of calcium oxide peaks (CaO, database card no. 7200686, green lines under the XRD peaks; **Figure 6**). The amorphous FeOOH decomposition led to the formation of crystalline hematite (Fe_2O_3, database card no. 9015065, brown lines under the XRD peaks; **Figure 6**), whose peaks are visible in the XRD spectrum (Cornell 2007). The XRD results demonstrate that the newly engineered FEZ adsorbent was successfully prepared.

4.5. Adsorption Properties

4.5.1. Effect of Adsorbent

Nickel removal efficiency and adsorption capacity of EZ and FEZ were examined as a function of adsorbent mass **(Figure 7A** and **7B)**.

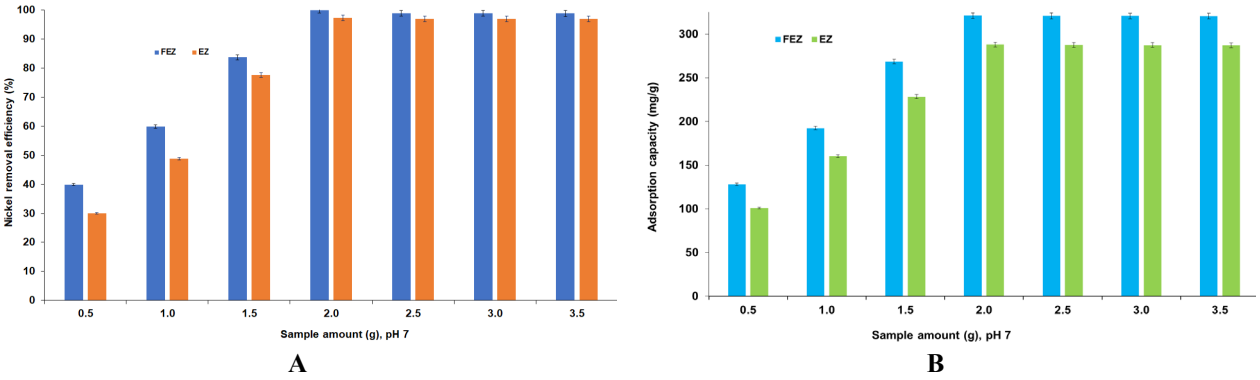

Figure 7. Nickel removal efficiency (**A**), and adsorption capacity (**B**) as a function of adsorbent mass

The diagrams show an increase in nickel adsorption with adsorbent amount rising from 0.50 g to 2.0 g. Adsorption reaches a maximum at 2.0 g of adsorbent (99.9% and 321.1 mg/g for FEZ, and 97.3% and 287.9 mg/g for EZ, respectively). After reaching equilibrium, adsorption shows a slight downward trend with increasing amounts of adsorbent. The results indicate that increasing adsorbent mass ensures greater availability of active sites until equilibrium is reached. After that, boosting adsorbent mass leads to agglomeration, thus decreasing the specific surface area and the active sites (Argun 2008; Al-Abbad, Al Dwairi 2021; Lei 2019; Mohan, Gandhimathi 2009).

4.5.2. Effect of initial concentration on nickel removal efficiency

The initial pollutant concentration represents one of the main driving forces of the adsorption process. To that end, the effect of the initial heavy metal concentration on nickel removal efficiency and adsorption capacity was investigated (**Figure 8A** and **8B**).

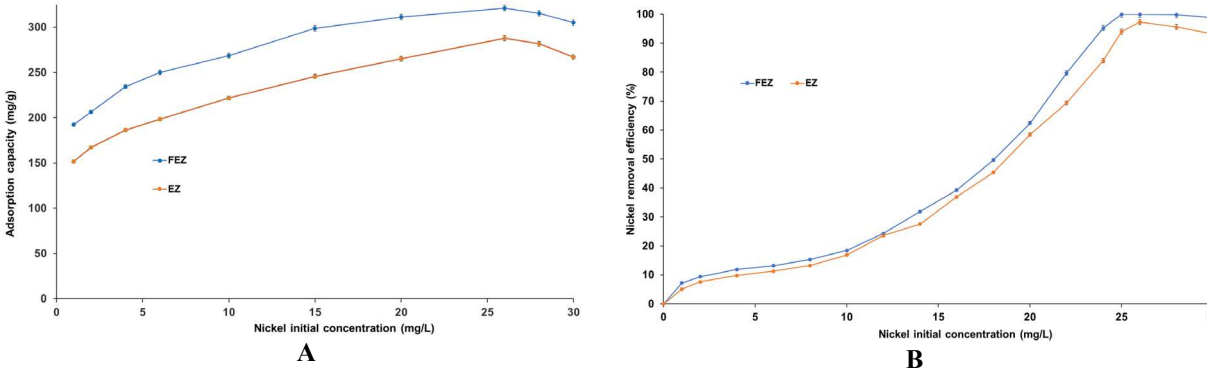

Figure 8. Relationship between nickel **(A)** initial concentration and adsorption capacity (mg/g), and **(B)** initial concentration and nickel removal efficiency (%)

It can be seen that removal efficiency shows direct proportional dependence on the increase of the initial concentration of the pollutant, in the range 0-30 mg/L, for both adsorbents (FEZ, EZ) (**Figure 8B**). **Figure 8A** shows that the adsorption capacities for FEZ and EZ exhibit an increasing trend in the same range of the initial pollutant concentration, 0-26 mg/L, reaching a maximum of 321.1 mg/g for FEZ and 287.9 mg/g for EZ.

Maximum removal efficiencies for FEZ (99.9%) and EZ (97.3%) were obtained at Ni(II) concentrations of 25.5 mg/L (**Figure 8B**). Past that point, both removal efficiencies follow a slightly decreasing trend. The same trend is observed for the adsorption capacities. According to collision theory, these results indicate that increase of nickel concentration (and implicitly the number of nickel ions) leads to an increase in the reaction rate due to numerous possibilities of interaction with acceptor sites on FEZ and EZ, until the equilibrium concentration has been reached (Fulazzaky 2011). Past the equilibrium point, an imbalance between a large number of nickel ions and a progressively decreasing number of active sites available on the adsorbents causes a decrease in the adsorption potential both in the case of FEZ and EZ. The obtained results corroborate the data reported for the component materials of the adsorbents (Annane 2021; Al-Abbad, Al Dwairi 2021; Noble, Terry 2004).

4.5.3. Effect of pH

pH is the parameter with a dominant effect on the adsorption process, because it influences the degree of ionic chemical speciation of the adsorbing species and adsorbent surface (Argun 2008; Chen 2016; Hosseini 2015; Kara, Demirbel 2011; Lei 2019; Zhai, Li 2019). In view of the aforementioned grounds, nickel ion adsorption on FEZ and EZ was investigated as a function of pH. To that end, the relationship between pH and nickel removal efficiency, as well as adsorption capacity, are shown in **Figure 9A** and **9B**.

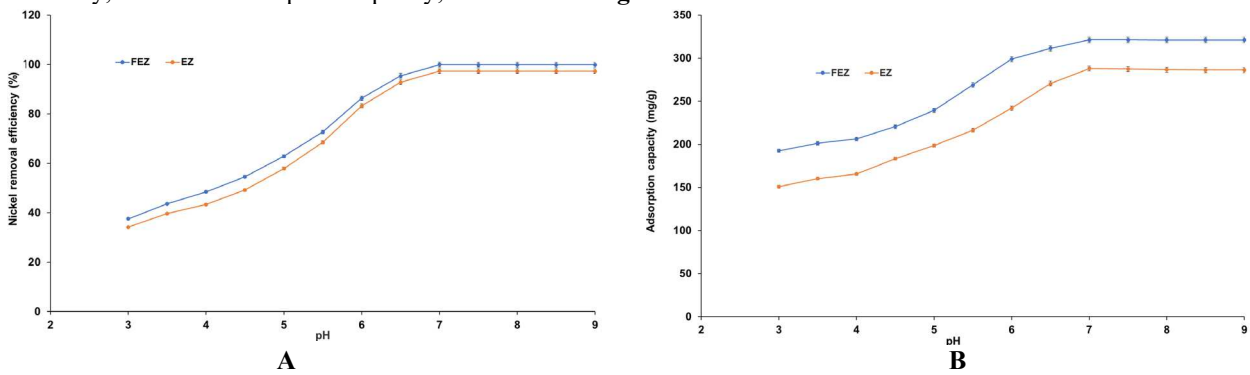

Figure 9. Effect of pH variation on **(A)** nickel removal efficiency, and (**B**) adsorption capacity

The results show that increase in pH from 3.0 to 7.0 induces a significant increase in the adsorbed nickel ions per unit mass of adsorbent. The adsorption efficiency and adsorption capacity reach a maximum value (99.9% and 321.1 mg/g for FEZ, and 97.3% and 287.9 mg/g for EZ) at pH 7.0, after which no further changes occur. It appears, therefore, that in an acidic environment, there is competition between protons and nickel cations for active sites available in the adsorbent. Moreover, boosting positive charge density on the adsorbent surface induces an electrostatic repulsion force on nickel ions. Consequently, the adsorption rate is low in an acidic environment. When pH increases, both the competing effect of protons and the electrostatic repulsion forces decrease, with the nickel ions increasingly occupying active sites in the adsorbent, thus increasing nickel removal efficiency (Argun 2008; Chen 2016; Hosseini 2015; Kara, Demirbel 2011; Lei 2019; Zhai, Li 2019).

At pH>7.0, generation of hydroxide ions prevails, with $[Ni(OH)]^+$ being the dominant species causing deceleration of the metal ion removal rate. Therefore, pH 7 was selected as the optimal value for further experiments. The emerging results are in good agreement with the reported data for the starting component materials used in adsorbent preparation (Argun 2008; Chen 2016; Hosseini 2015; Kara, Demirbel 2011; Lei 2019; Zhai, Li 2019).

4.5.4. Effect of contact time

The time required for adsorption of a pollutant is a critical factor, on which the cost of the adsorption process depends heavily (Argun 2008; Al-Abbad, Al Dwairi 2021; Lei 2019; Ma 2018). Nickel ion uptake capacities were determined as a function of contact time to establish an optimum contact time, at which the adsorption capacity and pollutant removal efficiency are maximized for each of the two adsorbents studied. The results (**Figure 10A** and **10B**) show that removal efficiency and adsorption capacity increase with increasing contact time for both investigated adsorbents.

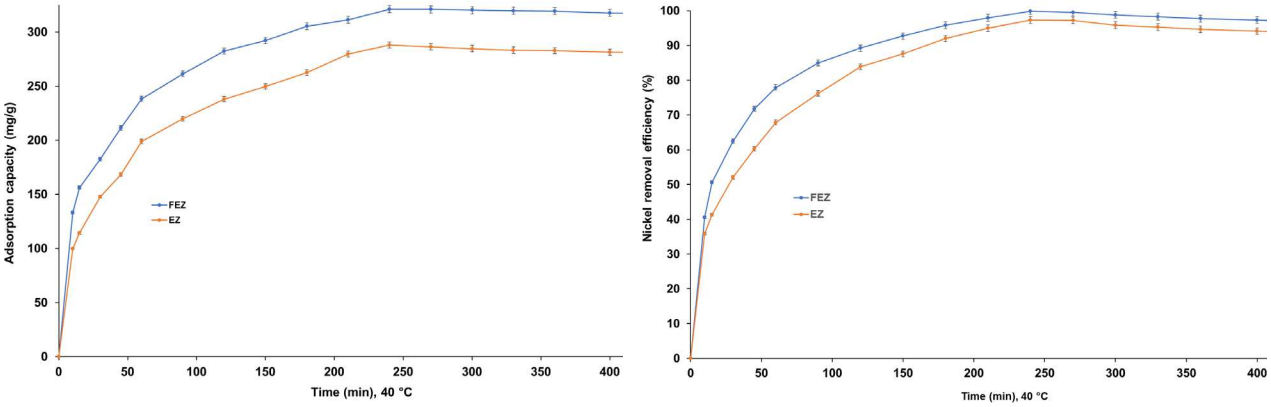

A **B**

Figure 10. Effect of contact time on (**A**) nickel adsorption capacity, and (**B**) nickel removal efficiency

Moreover, equilibrium is reached at 240 min, with a maximum adsorption capacity of 321.1 mg/g for FEZ and 287.9 mg/g for EZ. Also, at this time point, nickel removal efficiency reaches a maximum of 99.9% for FEZ and 97.3% for EZ. Further careful observation of the data suggests that there are three clear stages, in which nickel adsorption takes place:

a) in the first stage (0-120 min), adsorption increases rapidly, a phenomenon that could be attributed to the high availability of active sites in the adsorbent;

b) in the second stage (120-240 min), attenuation of the adsorption rate occurs, as a result of the decrease of available active sites;

c) in the third stage (240-460 min), metal adsorption exhibits a plateau trend, indicating saturation of the active sites, after reaching equilibrium. The data suggest that the optimal time necessary for the adsorption process to reach equilibrium for each of the adsorbents is 240 min.

4.5.5. Effect of temperature on adsorption process

Temperature is a significant parameter in the adsorption process, influencing the performance of an adsorbent (Kara, Demirbel 2011). Nickel uptake by FEZ and EZ adsorbents was investigated in the temperature range 5-50°C (**Figure 11A** and **11B**).

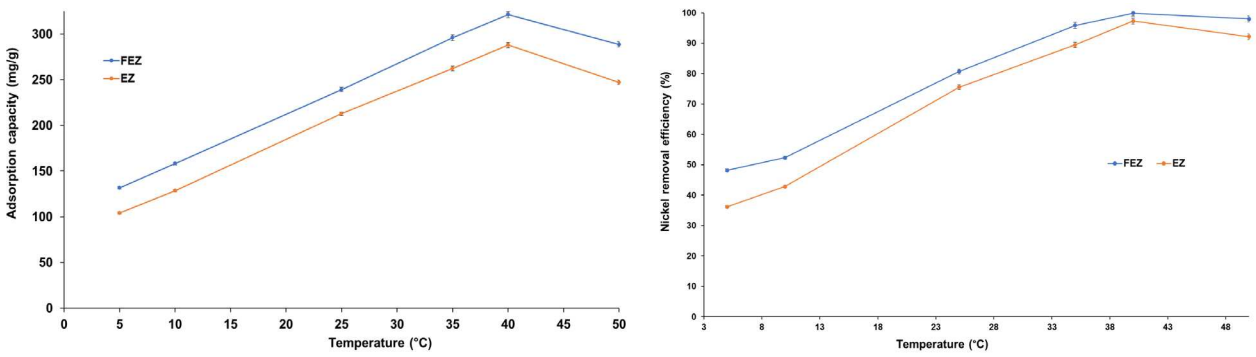

A **B**

Figure 11. Relationship between (**A**) temperature and adsorption capacity, and (**B**) temperature and nickel removal efficiency

The results show that adsorption is endothermic. Thus, it can be observed that nickel removal efficiency and adsorption capacity increase almost linearly with increasing temperature, up to a maximum, after which there is a slight decrease with increasing temperature. Maximum removal efficiency is reached at 40°C (99.9% for FEZ and 97.3% for EZ). At this temperature, a maximum nickel adsorption capacity of 321.1 mg/g for FEZ and 287.9 mg/g for EZ are observed. The data indicate that this temperature range is advantageous for increasing the mobility of metal ions and implicitly the interaction with acceptor sites on the adsorbent. To that end, the effect of temperature on the nickel adsorption process suggests that in the 5-40°C range, adsorption is an endothermic process in which physical adsorption takes place. At temperatures higher than 40°C, the chemisorption process occurs. However, it should be noted that even at 50°C very high removal efficiency values (>90%) are obtained for both adsorbents (97.9% for FEZ and 92.2 for EZ), thereby suggesting that a temperature increase beyond 40°C has a minimal effect on the adsorption process.

4.5.6. Nickel removal efficiency - comparative analysis between adsorbent and starting materials

Comparison of FEZ Ni(II) removal efficiency with EZ (before functionalization with FeOOH) and the starting materials (eggshell and zeolite), as a function of the contact time, was carried out. **Figure 12** shows that nickel removal efficiency increases with contact time for all four adsorbents: FEZ, EZ, eggshell, and zeolite.

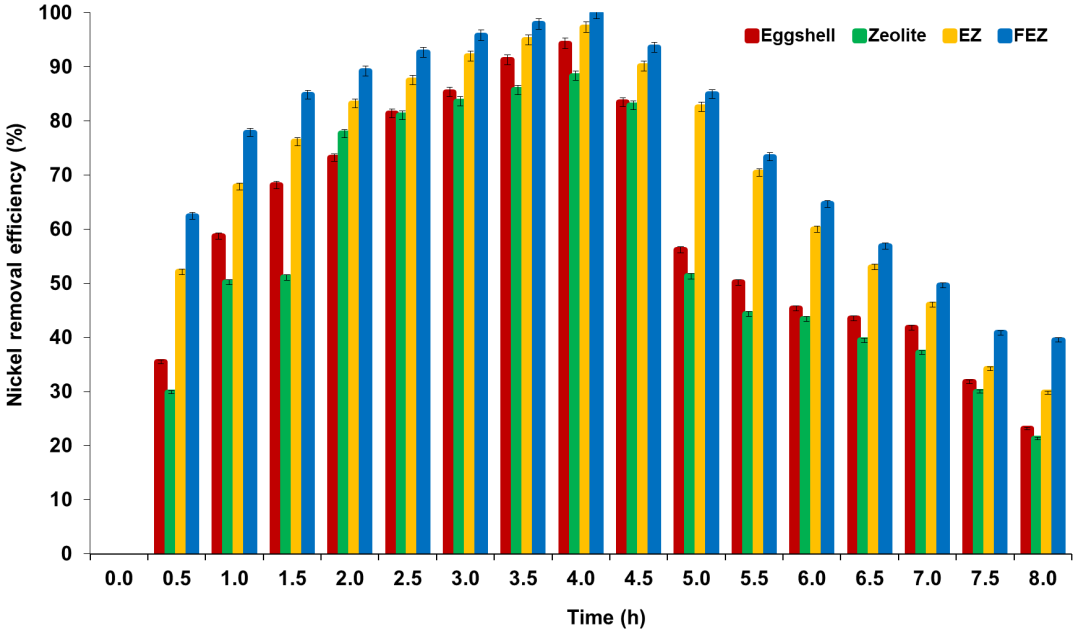

Figure 12. Removal efficiency and contact time relationship for all four adsorbents

Maximum efficiency is recorded at four hours, thus pointing to adsorption equilibrium. The experimental results show that pollutant removal efficiency decreases in the following order: FEZ (99.9%)>EZ (97.3%)>eggshell (94.3%) >zeolite (88.3%). After equilibrium has been reached, the adsorption rate decreases with increasing contact time. The data confirm the fact that adsorbent performance depends on the specific surface and porosity (BET

analysis in **Table 1**). The adsorption efficiency values for eggshell and zeolite samples are similar to those reported in the literature (Argun 2008; De Angelis 2017; Hosseini 2015; Zendelska 2018).

4.5.7. Adsorption Isotherms

Adsorption isotherms were perused to analyse nickel partition between the adsorbent and solution at equilibrium. The Langmuir and Freundlich models are the most common and reliable models to determine the maximum nickel adsorption capacity through adsorption isotherms (Annane 2021;Ayawei 2017; Mnasri-Ghnimi, Frini-Srasra 2019). Several studies have reported that nickel adsorption on eggshell, clinoptilolite or zeolite adsorbents fit the Langmuir and Freundlich adsorption isotherms (Al-Haj, El-Bishtawi 1997; Al Dwairi, Al-Rawajfeh 2012; Annane 2021; Khelifi 2016; Rajic 2010). Various studies have reported that the adsorption isotherms of Ni(II) on eggshell or zeolite (the primary materials from which the ZEF and EZ adsorbents were prepared), using the mathematical equations of Temkin and Dubinin-Radushkevich (D-R) adsorption models, do not fit well the experimental results (Al-Abbad, Al Dwairi 2021; Al Dwairi, Al-Rawajfeh 2012; Annane 2021; De Angelis 2017; Khelifi 2016; Krishna Kumar 2022; Mignardi 2020). Therefore, Langmuir and Freundlich adsorption isotherms were considered to adopt a suitable adsorption model adequate to reproduce the experimental results of this study (Ayawei 2017).

The Langmuir model is based on the theoretical principles that i) the adsorbent has a single, homogeneous layer, in which the adsorption process takes place, and ii) each of the adsorbed molecules has the same adsorption energy without contact between these molecules (Al Dwairi, Al-Rawajfeh 2012; Ayawei 2017).

The linear form of Langmuir model is expressed through the following equation (**eq. 4**)

$$\frac{C_e}{Q_e} = \frac{1}{kQ_m} + \frac{C_e}{Q_m} \quad \textbf{(eq. 4)}$$

In the Langmuir equation, the characteristic adsorption behavior can be calculated according to the following equation (**eq. 5**):

$$R_L = \frac{1}{1+kC_0} \quad \textbf{(eq. 5)}$$

where k (L/mg) is the Langmuir adsorption constant.

The Freundlich model is suitable to describe the multilayer adsorption process on the heterogeneous surface with non-uniform dispersion of heat and the interaction between the adsorbed molecules (Annane 2021; Chen 2016). In fact, the Freundlich isotherm was used to describe Ni(II) adsorption on the FEZ and EZ adsorbents, taking into consideration the distribution of energy sites and the competition between different ions for the adsorbent active sites available (Darweesh 2022; Mnasri-Ghnimi, Frini-Srasra 2019; Ouyang 2019).

The linear form of the Freundlich model is given by the equation below (**eq. 6**)

$$\log Q_e = \log k_f + \frac{1}{n} \log C_e \quad \textbf{(eq. 6)}$$

where k_f (mg/g) and n (g/L) are the constants of the Freundlich isotherm.

The plotted experimental data, using the linearized form of Langmuir and Freundlich models, are shown in **Figure 13A** and **13B**.

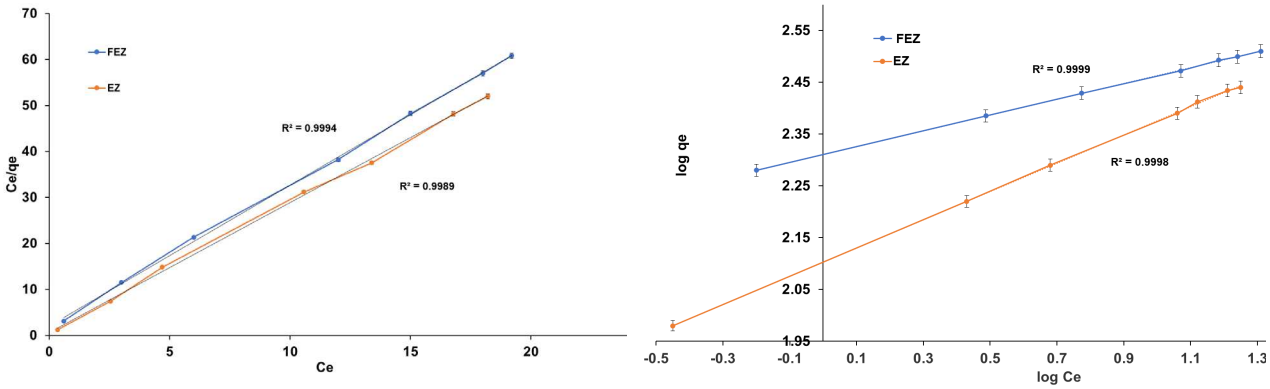

A **B**

Figure 13. Plot of the experimental data using the linearized form of **(A)** Langmuir model**,** and **(B)** Freundlich model

The calculated parameters of the two isotherms are presented in the **Table 2**.

Table 2. The Langmuir and Freundlich model parameters for nickel adsorption on ZEF and EZ.

Adsorbent material	Langmuir model					Freundlich model			
	$Q_{e,exp}$	Q_m	k	R_L	R^2	K_F	*n*	R^2	E_a (kJ/mol)

ZEF	321.1	321.0	0.283	0.861	0.9994	4.60517	1.893	0.9999	32.4
EZ	287.9	286.8	0.223	0.783	0.9989	3.85721	1.659	0.9998	32.2

Analysis of the isotherm data in **Table 2** indicates that both models provide satisfactory descriptions of nickel absorption on FEZ and EZ. The calculated maximum values of the adsorption capacity (Q_m) for the two considered adsorbents (FEZ and EZ) are in excellent agreement with those established experimentally at equilibrium ($Q_{e,exp}$) for the components of the newly prepared adsorbents (Annane 2021; Darweesh 2022; De Angelis 2017; Ouyang 2019; Wang 2021). The applicability of these two equilibrium models in describing the adsorption process for each of the two prepared adsorbents, EZ and FEZ, was evaluated based on the value of the correlation coefficient, R^2. Actually, the R^2 value obtained from the Freundlich model is slightly higher than that derived through the Langmuir model, suggesting that nickel ion adsorption is a multi-molecular layer adsorption process on irregular surfaces (Argun 2008; Rajic 2010).

The values of the equilibrium parameter from the Langmuir isotherm, R_L, were found to be in the range $0<R_L<1$ for EZ and FEZ, thus indicating a favorable adsorption process (Al Dwairi, Al-Rawajfeh 2012; Ayawei 2017; Nordstrand, Dutta 2019). In addition, according to the data from **Table 2**, the values of the Freundlich constant n, which provides information about the linearity of the adsorption, are higher than 1, thus suggesting a suitable physical adsorption process occurring on the investigated EZ and FEZ adsorbent heterogeneous surfaces (Ayawei 2017; Mignardi 2020; Nordstrand, Dutta 2019).

4.5.8. Thermodynamic study

The thermodynamic profile ascertaining the feasibility of EZ and FEZ as adsorbents for nickel removal was investigated. Assessment of the adsorbent thermodynamic behavior included the following parameters: Gibbs free energy (ΔG°), entropy (ΔS), and enthalpy (ΔH), determined according to Gibbs–Helmholtz and van't Hoff equations (**eq. 7** and **eq. 8**):

$$\Delta G^0 = -RT \ln K \qquad \textbf{(eq. 7)}$$

$$\ln K = \frac{-\Delta H^0}{RT} + \frac{\Delta S^0}{R} \qquad \textbf{(eq. 8)}$$

where,
K (mL/g) = adsorption equilibrium constant
ΔG^0 (kJ/mol) = free energy variation of the adsorption process
ΔH^0 (kJ/mol) = the standard enthalpy variation
ΔS^0 [J/(mol K)] = standard entropy variation
R = 8.314 J/(mol K) = the gas constant
T(K) = the absolute temperature.

Experiments were run at three different temperatures (295.15K, 303.15K, and 313.15K), at constant pH 7, using a 25.5 mg/mL nickel stock solution.

Van't Hoff's plot for the adsorption of nickel on FEZ and EZ is shown in **Figure 14**. The slope and intercept correspond to the thermodynamic parameters ΔH^0 and ΔS^0 (**Table 3**).

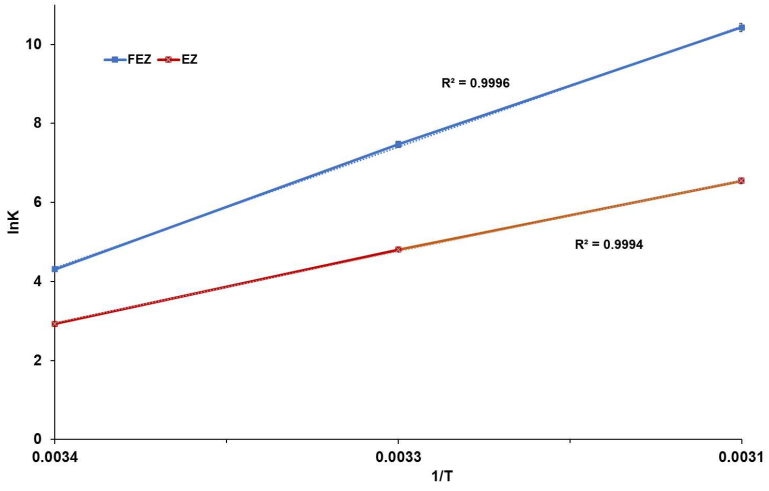

Figure 14. Van't Hoff plot for nickel adsorption on FEZ and EZ

Table 3. Thermodynamic parameters for adsorption nickel on EZ and FEZ adsorbents*

T(K)	Adsorbents					
	FEZ			EZ		
	ΔG^0 (kJ/mol)	ΔH^0 (kJ/mol)	ΔS^0 J/(mol K)	ΔG^0 (kJ/mol)	ΔH^0 (kJ/mol)	ΔS^0 J/(mol K)
295.15	-10.50	28.89	154.35	-7.14	24.61	138.32
303.15	-18.83			-12.12		
313.15	-27.15			-17.03		

* standard deviation (SD) = 0.02%

Negative ΔG^0 values indicate thermodynamic feasibility and spontaneity of the prepared adsorbents for nickel removal in the employed temperature range. ΔH^0 provides information on the physical or chemical nature of the adsorption process (28.89 kJ/mol for FEZ and 24.61 kJ/mol for EZ), reflecting an endothermic adsorption process, with a favorable affinity of nickel for the two adsorbents (Al-Abbad EA, Al Dwairi 2021; Krishna Kumar 2022; Mnasri-Ghnimi, Frini-Srasra 2019). Positive ΔS^0 values denote adsorbent (FEZ and EZ) affinity for nickel ions and indicate that the adsorption could involve structural changes (Al-Abbad EA, Al Dwairi 2021; Krishna Kumar 2022; Mnasri-Ghnimi, Frini-Srasra 2019; Sahmoune 2019).

4.5.9. Adsorption kinetic study

Several mechanisms can control an adsorption process: mass transfer, particle diffusion, diffusion control or chemical reactions. To that end, kinetic studies were launched to obtain information on adsorbent effectiveness, insight into the adsorbent process (mass transfer), and dynamic parameters of adsorption (rate, temperature) (Mnasri-Ghnimi S, Frini-Srasra 2019; Wang, Guo 2020). In that respect, a pseudo-first-order kinetic model, a pseudo-second-order kinetic model, and an intraparticle diffusion model were applied to test the experimental data on nickel adsorption for the newly prepared adsorbents FEZ and EZ.

The pseudo-first-order kinetic model (Lagergren equation) assumes that the adsorption rate depends on the number of active sites available (Ebelegi 2020).

The linear form of the Lagergren equation is expressed as follows (**eq. 9**):

$$\ln (Q_e - Q_t) = lnQ_e - k_1 t \qquad \textbf{(eq. 9)}$$

where Q_e (mg/g) and Q_t (mg/g) represent the adsorption capacities at equilibrium and at time t, respectively, with k_1 (min^{-1}) being the rate constant of adsorption kinetics.

The pseudo-second-order model assumes that the adsorption rate depends on the existence of chemical interactions between the nickel ions and the functional groups on the adsorbent (Ebelegi 2020).

The linearized form of the second-order kinetics is presented in the following equation (**eq. 10**):

$$\frac{1}{Q_t} = \frac{1}{K_2\ Q_e^2} + \frac{1}{Qe}\ t \qquad \textbf{(eq. 10)}$$

where k_2 [mg/(g min)] is the rate constant of the pseudo-second-order kinetics.

The Weber and Morris intraparticle diffusion model hypothesizes that diffusion of nickel ions through adsorbent pores influences the adsorption rate. The Weber and Morris model is described as follows (**eq. 11**):

$$Q_t = k_i t^{1/2} + C \quad \textbf{(eq. 11)}$$

where k_i [mg/(g $min^{-1/2}$)] is the intraparticle diffusion rate constant and C (mg/g) is a constant related to the thickness of the boundary layer.

Figure 15A-C shows the plots of the kinetics models for nickel adsorption on FEZ and EZ.

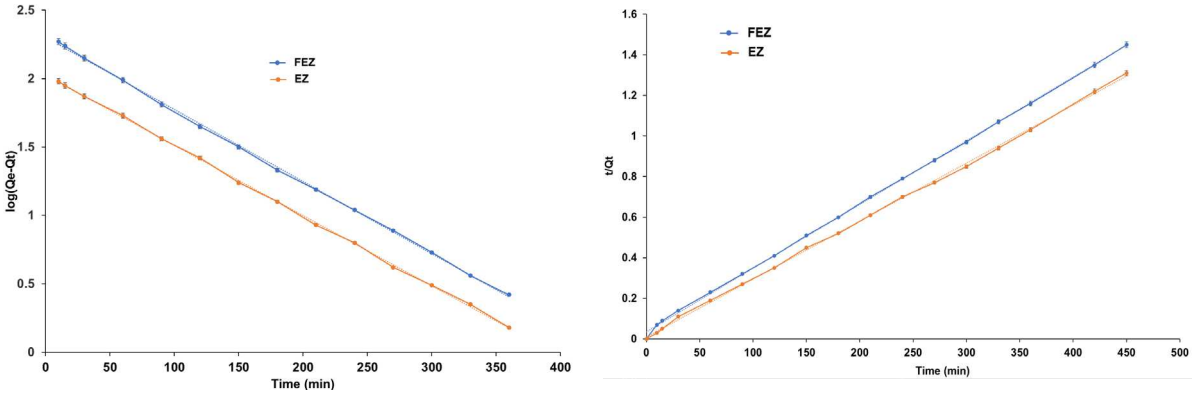

A **B**

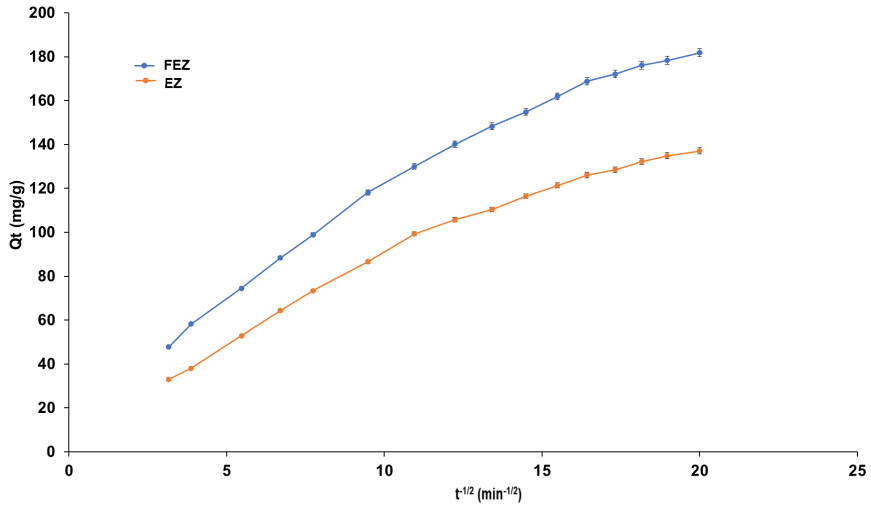

C

Figure 15. (**A**) Pseudo-first-order model fitting diagram, (**B**) Pseudo-second-order model fitting diagram, and (**C**) Intraparticle diffusion model fitting diagram

The kinetic constants were determined from the slopes and intercepts of these diagrams (**Table 4**).

Table 4. Kinetic parameters for nickel adsorption on FEZ and EZ adsorbents*

Adsorbent material	q_e^{exp} (mg/g)	Pseudo first order			Pseudo second order			Intraparticle diffusion		
		q_e^{calc}	K_1	R^2	q_e^{calc}	K_2	R^2	K_i	C	R^2
FEZ	321.1	322.28	0.023	0.9994	321.58	2.781	0.9997	8.0276	33.875	0.9764
EZ	287.9	288.35	0.011	0.9991	287.95	1.924	0.9993	6.2782	21.466	0.9726

* standard deviation (SD) = 0.02%

The data reveal insignificant differences between the values of the correlation coefficients of the pseudo-first-order and pseudo-second-order kinetic models. That could indicate that retention of nickel on the adsorbents is achieved through a chemical and physical adsorption process. However, it can be seen that the calculated values of the adsorption capacity at equilibrium are much closer to the experimental ones obtained in the case of the pseudo-second-order kinetics model. In other words, nickel ion adsorption on the adsorbents relies mainly on chemisorption, involving chemical bond formation between nickel ions and active sites (Al-Abbad, Al Dwairi 2021; Annane 2021; Argun 2008; De Angelis 2017; Mignardi 2020). The correlation coefficient for the intraparticle diffusion model is higher than 0.97 for both adsorbents, suggesting that intraparticle diffusion is involved in the adsorption process. However, intraparticle diffusion could not be the only rate-limiting step, because the diagram is not linear and deviates from the origin point (De Angelis 2017). The kinetics results corroborated the data reported in the literature for the starting materials of the proposed adsorbents (Al-Abbad, Al Dwairi 2021; Annane 2021; Argun 2008; De Angelis 2017; Mignardi 2020).

4.5.10. Insight into adsorption

Evaluation of structural and morphological changes through FT-IR and SEM-EDX techniques was used to investigate potential nickel adsorption mechanisms on both proposed materials. Comparative assessment of FT-IR spectra of the proposed adsorbents EZ and FEZ was performed before and after nickel removal, in order to reveal changes occurring in the adsorbents.

The FT-IR spectrum of EZ after nickel retention (**Figure 5SA**) shows a shift of some adsorption peaks and the emergence of new bands. Thus, shifts to higher energies of the adsorption bands from 469 (Si-O-Si vibrational deformation) to 487 cm^{-1}, 797 cm^{-1} (Si-O) to 802 cm^{-1}, 3480 cm^{-1} (OH vibrations) to 3491 cm^{-1}, and 3625 cm^{-1} (Si-OH-Si or Al-OH-Al) to 3632 cm^{-1} were observed (**Figure 5SA** and **5SB**). These changes can be attributed to chemical interactions between nickel ions and the corresponding functional groups. Following nickel removal, the EZ spectrum shows the appearance of adsorption bands at 487, 668, and 1449 cm^{-1}. The peak at 487 cm^{-1} can be attributed to α-$Ni(OH)_2$ and the peak at 668 cm^{-1} can be attributed to the Ni–O stretching vibration mode (Hall 2015; Qiao 2009) The weak band at 1449 cm^{-1} can be assigned to chloride ions from the heavy metal source (nickel chloride) (Chen 2003).

Assessment of the FT-IR spectra of FEZ (**Figure 6SA** and **6SB**) before and after Ni(II) removal depicted a series of notable differences (intensity of vibrational peaks, displacement or appearance of new absorption bands).

Substantial changes of the O-H features at ~3437 cm^{-1} and 1636 cm^{-1} indicate that this functional group participates in the heavy metal adsorption process (Pang 2022; Xin 2018; Zhai, Li 2019). An increase in intensity of the bands at 1423 and 876 cm^{-1} (C-O stretching vibration), 2511 cm^{-1} (O-C-O), and 2976 cm^{-1} (C-H symmetric and antisymmetric stretching vibrations) can also be observed. These changes can be attributed to the interaction of nickel ions with the functional groups of the FEZ adsorbent (Argun 2008).

The FT-IR spectra of FEZ after adsorption show that the peaks at ~630 cm^{-1} (Fe–O stretch), 797 cm^{-1} (attributed to Si-O), 872 cm^{-1} (corresponding to C-O stretching vibration), 1055 cm^{-1} (assigned to Si-O stretching vibration), 2517 cm^{-1} (attributed to O-C-O), and 2974 cm^{-1} (associated with C-H symmetric and antisymmetric stretching vibration) have been shifted.

The new absorption bands at 472 cm^{-1} and 665 cm^{-1} can be attributed to α-$Ni(OH)_2$ and Ni–O stretching vibration modes, respectively (Hall 2015; Sharma 2014; Qiao 2009). An increase in intensity of the peak at ~608 cm^{-1} can be attributed to the overlap of the Ni–O stretching band (Hall 2015; Sharma 2014; Qiao 2009). Also, the weak band at 1460 cm^{-1} can be assigned to chloride ions from the heavy metal source (nickel chloride) (Chen 2003). Collectively, the FT-IR results suggest that nickel adsorption on FEZ proceeds through chemical bond formation (Gorzin, Bahri Rasht Abadi 2017; Nasehi 2019).

Morphological changes (particle and pore size, shape, particle distribution) on the structure of both EZ and FEZ after nickel adsorption were also investigated by SEM-EDX **(Figure 7S-8S**) to corroborate the FT-IR spectroscopy results. The SEM micrograph of EZ material after nickel adsorption (**Figure 7SA-D**) indicates the presence of numerous particles of irregular shapes attributed to the pollutant. Also, after nickel adsorption, the SEM image of FEZ (**Figure 8SA-E**) shows the appearance of several particles of nanometric sizes and irregular shapes. On the other hand, SEM (**Figure 7S-8S**) indicates a decrease in porosity after nickel adsorption for both proposed materials. These changes in adsorbent morphology suggest that, under the employed experimental conditions, the dissolution-precipitation phenomenon plays a dominant role in the nickel adsorption mechanism (De Angelis 2017; Mignardi 2020).

Elemental analysis and distribution in FEZ and EZ after nickel adsorption was examined through SEM live maps (**Figure 9SA-B**) and EDX analysis (**Figure 10SA-B**). It appears that there are differences in the amount of nickel retained on the EZ surface compared to FEZ. In fact, nickel identified in FEZ was much higher than in EZ. By the same token, after nickel adsorption, elemental composition of FEZ and EZ through EDX analysis (**Figure 10SA-B**) indicates the presence of a peak corresponding to the heavy metal (**Figure 10SA-B**), thus confirming nickel adsorption (Gorzin, Bahri Rasht Abadi 2017; Khan 2021).

4.5.11. Comparison of nickel removal efficiency with other adsorbents

Adsorption performance comparison of the two prepared adsorbents with others reported in the literature on nickel removal is presented in **Table 5**.

Table 5. Comparison of nickel removal efficiency of adsorbents EZ and FEZ with the literature (selected study) on materials similar to EZ and FEZ components

Adsorbent type	Removal efficiency (%)	Literature Reference
eggshell	90.9	(Ho 2014)
eggshell	93.5	(Mashangwa 2016)
eggshell-derived hydroxyapatite	91.0	(De Angelis 2017
vinegar-treated eggshell waste biomass	76.5	(Stevens, Batlokwa 2017)
clinoptilolite	93.6	(Argun 2008)
zeolite	58.6	(Al-Abbad, Al Dwairi 2021)
supported zeolite-Y hollow fiber membranes	63.0	(Muhamad 2018)
clinoptilolite	60.0	(Ismail 2012)
EZ	97.3	This study
FEZ	99.9	This study

The results indicate that the two new adsorbents EZ and FEZ have a much higher adsorption efficiency than any other known materials. That could be attributed to the higher surface area compared to their components (eggshell or zeolite), following adsorbent surface modification.

4.5.12. Desorption study and adsorbent regeneration

Cycling stability is essential to high-performance and economic feasibility for an adsorbent (Qasem 2021). Regeneration efficiency depends on the ease with which the desorption process of the adsorbed pollutant takes place (Kara, Demirbel 2011). Consequently, nickel ion desorption under acidic (nitric acid and hydrochloric acid) and alkaline (sodium hydroxide) conditions was investigated (**Figure 16A**). The results suggest that in an acidic environment, the desorption rate increases proportionally in the time range of 0-11 h, reaching the maximum value. After this point, a decrease in desorption yield with time is observed.

The desorption rate was 91% in FEZ and 89% in EZ (**Figure 16A**), when 0.1 M HNO_3 was used as desorption agent. When 0.1 M HCl was used instead, over 80% of the heavy metal was desorbed from both adsorbents. This result can be attributed to the generation of abundance of protons, thereby determining an exchange between the adsorbed nickel ions and protons and the protonation of the functional groups in the adsorbent (Charazińska 2022). However, in an alkaline medium, desorption rates of ~2% can be justified by the existence of two competing phenomena: nickel precipitation and the negative charge of the functional groups in the adsorbents, which favors adsorption (pH 6-9) more than nickel ion desorption (Olad 2013). To that end, thirteen cycles of nickel adsorption and desorption processes on both adsorbents were run to investigate their reusability potential. Nickel adsorption capacity variation on the two adsorbents, depending on the number of adsorption-desorption cycles, is shown in **Figure 16B**.

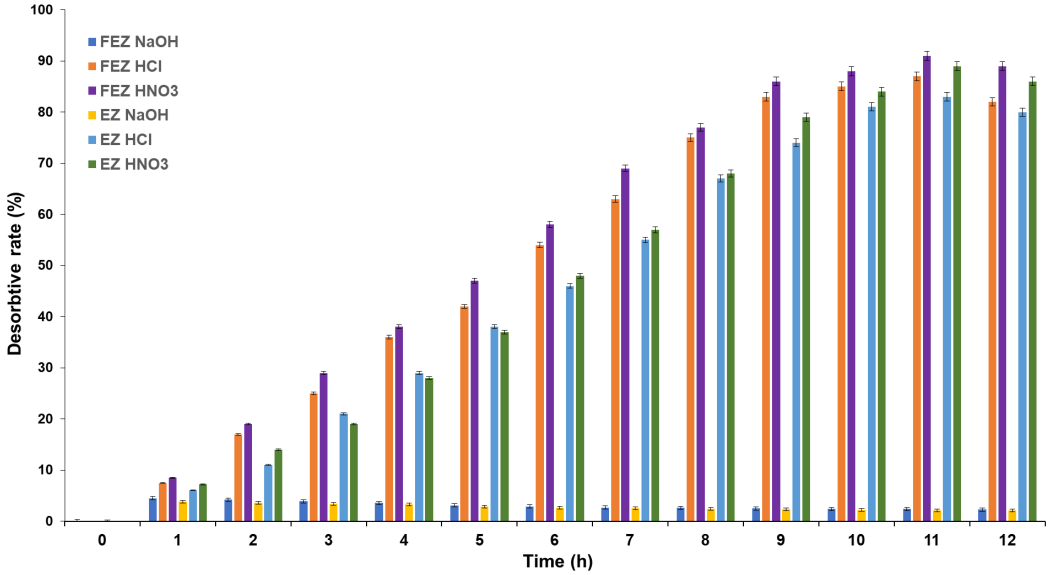

A

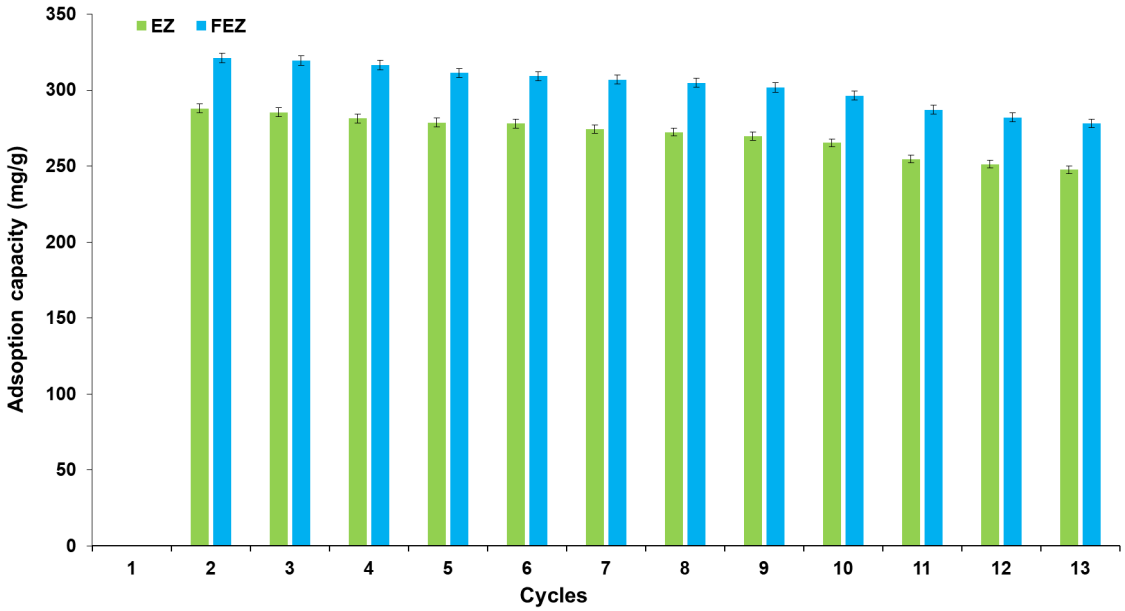

B

Figure 16. **(A)** Relationship between desorption rate and time, **(B)** Reusability of FEZ and EZ

After ten cycles, the adsorption capacity barely decreased by about 12% for EZ and 10.5% for FEZ. These results indicate that the performance and reusability of the two adsorbents are very high.

4. Discussion

We have demonstrated successful preparation of two new adsorbents engineered from eggshell waste and zeolite (EZ and FEZ). The second adsorbent (FEZ) preparation led to double functionalization of the eggshell with the zeolite nanoparticles, achieved simultaneously through loading of the eggshell pores and zeolite surface with α-FeOOH particles. The XRD spectrum of FEZ demonstrated that the α-FeOOH is in an amorphous state, which could explain FEZ's higher specific area and enhanced adsorption capacity compared to EZ. Both adsorbents can be used successfully to remove nickel from aqueous solutions. Their adsorption behavior follows the Freundlich isotherm and pseudo-second-order models. The adsorption efficiency of EZ allows removal of over 97% Ni(II) and more than 99% Ni(II) for FEZ. In contrast to the data reported for zeolite, eggshell or even functionalized eggshell, the two new adsorbents possess superior absorption capacity attributed to the higher surface, and the microporous structure resulting from the employed experimental conditions. In comparison to the literature on materials similar to their components, the herein reported new adsorbents (EZ and FEZ) exhibit higher adsorption efficiency (Annane 2021; Argun 2008; Chen 2016; De Angelis 2017; Gorzin, Bahri Rasht Abadi 2017; Ho 2014; Khan 2021; Mashangwa 2016; Nasehi 2019; Pang 2022).

In addition, the materials obtained in this work show environmental performance and ensure nickel recycling in different economically valuable forms. To that end, a) consecutively separated solutions containing nickel from the desorption process could be collected and used in nickel-plating baths, b) the saturated EZ and FEZ adsorbents could be used as raw materials in cement or ceramic materials production (Lysenko 2022; Sinyoung 2015), and c) the nickel-containing materials (EZ and FEZ after adsorption) could be used as fertilizers, considering the components of the newly prepared adsorbents together with the recognized role of nickel in nitrogen metabolism in plants (Patra 2020; Vischetti 2022). Congruent with such applications is the fact that both adsorbents show high cycling stability. After ten successive adsorption-desorption cycles, the adsorption efficiency of Ni(II) decreases by only approximately 10% for both adsorbents examined. Overall, the results reveal that these new adsorbents, prepared from waste, have merit in the remediation of wastewater in the context of sustainable economy.

5. Conclusions

The undertaken study describes nickel removal from an aqueous solution, using two newly engineered adsorbents, EZ and FEZ, prepared from eggshell waste, zeolite, and iron. The adsorption behavior and mechanism(s) were investigated through isothermal, thermodynamic, and kinetic models. The functionalization mechanism for the first adsorbent (EZ) involved loading the eggshell pores with zeolite particles, further confirmed by SEM, XRD, and FTIR techniques. In the case of the second adsorbent (FEZ), however, the functionalization mechanism involved simultaneous loading of each component (zeolite and eggshell) surface with α-FeOOH particles, to ensure considerable increase in sorption sites and surface area for heavy metal ions. XRD analysis demonstrated that α-FeOOH is in an amorphous state in this adsorbent (FEZ), thus explaining the increase in the specific surface area. SEM and BET support these structural changes occurring during FEZ preparation. Accordingly, the specific surface area increase allowed better adsorption performance for FEZ (99.9% and 321.1 mg/g) compared to EZ (97.3% and 287.9 mg/g). The best results for both adsorbents were obtained at 40°C, pH 7 and 240 min. The results of isotherm, thermodynamic and kinetics models indicate that retention of nickel on the two prepared adsorbents is achieved through a chemical adsorption process described by a second-order model. In addition, SEM and FT-IR studies after nickel adsorption suggest that nickel adsorption is achieved through chemical bond formation. The studies on the regeneration efficiency of the new adsorbents showed that nickel could be optimally desorbed from the surface of the adsorbents in the presence of nitric acid. The maximum desorption rate was 91% on FEZ and 89% on EZ. Collectively, the study shows that highly efficient and reusable adsorbents could be prepared through a simple functionalization method of eggshell waste using cheap and eco-friendly materials.

6. References

Al-Abbad EA, Al Dwairi RA (2021) Removal of nickel (II) ions from water by Jordan natural zeolite as sorbent material. Journal of Saudi Chemical Society 25(5): 101233.

Al Dwairi RA, Al-Rawajfeh AE (2012) Removal of cobalt and nickel from wastewater by using Jordan low-cost zeolite and bentonite, Journal of the University of Chemical Technology and Metallurgy 47(1):69-76.

Al-Haj AA, El-Bishtawi R (1997) Removal of lead and nickel ions using zeolite tuff, J. Chem. Tech. Biotechnol. 69: 27-34.

Alquzweeni SS, Alkizwini RS, (2020) Removal of cadmium from contaminated water using coated chicken bones with double-layer hydroxide (Mg/Fe-LDH). Water 12: 2303.

Aman T, Kazi AA, Sabri MU, Bano Q (2008) Potato peels as solid waste for the removal of heavy metal copper(II) from waste water/industrial effluent. Colloids and Surfaces B: Biointerfaces. 63(1): 116–121.

Annane K, Lemlikchi W, Tingry S (2021) Efficiency of eggshell as a low-cost adsorbent for removal of cadmium: kinetic and isotherm studies. Biomass Conversion and Biorefinery. Springer.

Argun ME (2008) Use of clinoptilolite for the removal of nickel ions from water: Kinetics and thermodynamics. Journal of Hazardous Materials. 150(3):587–595.

Ayawei N, Newton Ebelegi A, Wankasi D (2017) Modelling and interpretation of adsorption isotherms. Journal of Chemistry article ID 3039817, 11 pp.
Carvalho J, Araujo J, Castro F (2011) Alternative low-cost adsorbent for water and wastewater decontamination derived from eggshell waste: An overview. Waste Biomass Valor. 2: 157–167.
Charazińska S, Burszta-Adamiak E, Lochyński P (2022) Recent trends in Ni(II) sorption from aqueous solutions using natural materials. Rev Environ Sci Biotechnol 21: 105–138.
Chen D, Xiao X, Yang K (2016) Removal of phosphate and hexavalent chromium from aqueous solutions by engineered waste eggshell. RSC Advances. 6(42): 35332–35339.
Chen JY, Matsunaga R, Ishikawa K, Zhang H (2003) Determination of chloride ion concentration of concentrated-seawater using near Infrared Spectroscopy, Bull. Soc. Sea Water Sci. Jpn., 57: 491-497.
Chukanov NV, Chervonnyi AD (2016) IR Spectra of minerals and related compounds, and reference samples' data. In Infrared Spectroscopy of Minerals and Related Compounds. Springer Mineralogy. Springer, Cham.
Council Directive 98/83/EC of 3 Nov. on the quality of water intended for human consumption (1998) OJ L 330, 5.12.1998:1–28.
Cornell RM, Giovanoli R, Schneider W (2007) Review of the hydrolysis of iron(III) and the crystallization of amorphous iron(III) hydroxide hydrate. Journal of Chemical Technology & Biotechnology 46(2): 115–134.
Darweesh MA, Elgendy MY, Ayad MI, Ahmed AMM, Elsayed NMK, Hammad WA (2022) Adsorption isotherm, kinetic, and optimization studies for copper (II) removal from aqueous solutions by banana leaves and derived activated carbon, South African Journal of Chemical Engineering 40: 10-20.
De Angelis G, Medeghini L, Conte AM, Mignardi S (2017) Recycling of eggshell waste into low-cost adsorbent for Ni removal from wastewater. Journal of Cleaner Production, 164: 1497–1506.
Ebelegi AN, Ayawei N, Wankasi D. (2020) Interpretation of adsorption thermodynamics and kinetics. Open Journal of Physical Chemistry 10: 166-182.
El-Azazy M, El-Shafie AS, Issa AA, Al-Sulaiti M, Al-Yafie J, Shomar B, Al-Saad K (2019) Potato peels as an adsorbent for heavy metals from aqueous solutions: eco-structuring of a green adsorbent operating Plackett–Burman design, Journal of Chemistry 2019, Article ID 4926240, 14 pg.
El-Naggar A, Ahmed N, Mosa A, Niazi NK, Yousaf B, et.al., (2021) Nickel in soil and water: Sources, biogeochemistry, and remediation using biochar. Journal of Hazardous Materials. 419: 126421.
EFSA Panel on Contaminants in the Food Chain (CONTAM), Schrenk D, Bignami M, Bodin L, Chipman JK, Del Mazo J, Grasl-Kraupp B, Hogstrand C, Hoogenboom LR, Leblanc JC, Nebbia CS, Ntzani E, Petersen A, Sand S, Schwerdtle T, Vleminckx C, Wallace H, Guérin T, Massanyi P, Van Loveren H, Baert K, Gergelova P, Nielsen E (2020). Update of the risk assessment of nickel in food and drinking water. EFSA J. 18(11), e06268.
EPA- United States Environmental Protection Agency, Technical Documentation: Drought, 2021. https://www.epa.gov/climate-indicators/climate-change-indicators-drought. Accessed 28 December 2022.
European Commission, Communication from the Commission to the European Parliament, the Council. The European Economic and Social Committee and the Committee of the Regions (2015) Closing the loop -An EU action plan for the Circular Economy, Brussels, 2.12.2015. COM (2015) 614 final.
Fernández-Reyes B, Ortiz-Martínez K, Lasalde-Ramírez JA, Hernández-Maldonado AJ, (2020) Engineered adsorbents for the removal of contaminants of emerging concern from water. Contaminants of Emerging Concern in Water and Wastewater: 3–45.
Fulazzaky MA, (2011) Determining the resistance of mass transfer for adsorption of the surfactants onto granular activated carbons from hydrodynamic column. Chemical Engineering Journal 166(3): 832–840.
Genchi G, Carocci A, Lauria G, Sinicropi MS (2020). Catalano A, Nickel: human health and environmental toxicology. Int J Environ Res Public Health.17(3): 679.
Gorzin F, Bahri Rasht Abadi M (2017) Adsorption of Cr(VI) from aqueous solution by adsorbent prepared from paper mill sludge: Kinetics and thermodynamics studies. Adsorption Science & Technology 36(1-2):149–169.
Hall DS, Lockwood DJ, Bock C, MacDougall BR (2015) Nickel hydroxides and related materials: a review of their structures, synthesis and properties. Proc. R. Soc. A 471: 20140792.
Ho JH, Yeh YN, Wang HW, Khoo SK, Chen YH, Chow CF (2014) Removal of nickel and silver Ions using eggshells with membrane, eggshell membrane, and eggshells. Food Science and Technology Research 20(2): 337–343.
Hosseini SSS, Khosravi A, Tavakoli H, Esmhosseini M, Khezri S (2015) Natural zeolite for nickel ions removal from aqueous solutions: optimization and modeling using response surface methodology based on central composite design. Desalination and Water Treatment: 1–9.
Ismail, M.H.S., Zhang X.T., Adnan S.N. (2012) Application of clinoptilolite in removal of nickel (II) in plating wastewater, World Appl. Sci. J. 18(5), 659–664
Jai PH, Wook JS, Kyu YJ, Gil KB, Mok LS (2007) Removal of heavy metals using waste eggshell. Journal of Environmental Sciences. 19: 1436–1441.
Kaufhold S, Ufer K, Hein M, et al. (2022) A combined IR and XRD study of natural well crystalline goethites (α-FeOOH). Acta Geochim. 41: 794–810.

Kara A, Demirbel E (2011) Kinetic, isotherm and thermodynamic analysis on adsorption of Cr(VI) ions from aqueous solutions by synthesis and characterization of magnetic-poly(divinylbenzene-vinylimidazole) microbeads, Water, Air, & Soil Pollution 223(5): 2387–2403.

Khan MN, Ullah H, Naeem S, Uddin J, Hamid Y, Ahmad W, Ding J (2021) Remediation of emerging heavy metals from water using natural adsorbent: Adsorption performance and mechanistic insights. Sustainability 13: 8817.

Khelifi O, Nacef M, Affoune AM (2016) Biosorption of Nickel(II) ions from aqueous solutions by using Chicken eggshells as low-cost biosorbent, Algerian J. Env. Sc. Technology 2(1):107-111.

Krishna Kumar AS, Warchol J, Matusik J et al. (2022) Heavy metal and organic dye removal via a hybrid porous hexagonal boron nitride-based magnetic aerogel. npj Clean Water 5:24.

Lei T, Li SJ, Jiang F, et al. (2019) Adsorption of cadmium ions from an aqueous solution on a highly stable dopamine-modified magnetic nano-adsorbent. Nanoscale Res Lett. 14: 352.

Lyubchik S, Lygina E, Lyubchyk A, Lyubchik S, et al. (2016) The kinetic parameters evaluation for the adsorption processes at "liquid–solid" interface. Electrokinetics Across Disciplines and Continents: 81–109.

Lysenko VI (2022) Production and properties of ceramic made from nickel oxide nanopowder, Glass Ceram. 79: 9-10.

Ma L, Wei Q, Chen Y, Song Q, Sun C, Wang Z, Wu G (2018) Removal of cadmium from aqueous solutions using industrial coal fly ash-nZVI. R. Soc. Open Sci. 5:171051.

Mashangwa TD (2016) An investigation into the efficacy of eggshells as a low cost adsorbent for the removal of potentially toxic inorganic elements from aqueous solutions, Dissertation, Master of Science Dissertation, Environmental Science, University of South Africa.

Mignardi S, Archilletti L, Medeghini L et al. (2020) Valorization of eggshell biowaste for sustainable environmental remediation. Sci Rep. 10: 2436.

Mnasri-Ghnimi S, Frini-Srasra N (2019) Removal of heavy metals from aqueous solutions by adsorption using single and mixed pillared clays. Applied Clay Science. 179: 105151.

Mohan S, Gandhimathi R (2009) Removal of heavy metal ions from municipal solid waste leachate using coal fly ash as an adsorbent. Journal of Hazardous Materials 169(1–3): 351-359.

Muhamad N, Abdullah N, Rahman MA, et al. (2018) Removal of nickel from aqueous solution using supported zeolite-Y hollow fiber membranes. Environ Sci Pollut Res 25: 19054–19064.

Nakajima K, Nansai K, Matsubae K, Tomita M, Takayanagi W, Nagasaka T, (2017) Global land-use change hidden behind nickel consumption. Science of the Total Environment. 586: 730–737.

Nasehi P, Mahmoudi B, Abbaspour SF, Moghaddam MS (2019) Cadmium adsorption using novel $MnFe_2O_4$-TiO_2-UIO-66 magnetic nanoparticles and condition optimization using a response surface methodology. RSC Advances, 9(35): 20087–20099.

Noble RD, Terry PA, (2004) Adsorption. In Principles of chemical separations with environmental Applications, (Cambridge Series in Chemical Engineering, pp. 182-213). Cambridge: Cambridge University Press.

Nordstrand J, Dutta J (2019) Dynamic Langmuir model: A simpler approach to modeling capacitive deionization. J. Phys. Chem. C, 123(26):16479–1648.

Olad A, Ahmadi S, Rashidzadeh A (2013) Removal of nickel (II) from aqueous solutions with polypyrrole modified clinoptilolite: kinetic and isotherm studies. Desalination and Water Treatment 51(37-39): 7172–7180.

Öden MK, Karasakal EN, Çildir S (2022) Nickel (II) removal from synthetic wastewater by adsorption using waste pea shell, International Journal of Environmental Trends 6(1):10-20.

Ouyang D, Zhuo Y, Hu L, Zeng Q, Hu Y, et. al. (2019) Research on the adsorption behavior of heavy metal ions by porous material prepared with silicate tailings. Minerals 9(5): 291.

Parades-Aguilar J, Reyes-Martínez V, Bustamante G, Almendáriz-Tapia FJ, Martínez-Meza G, et.al. (2021) Removal of nickel(II) from wastewater using a zeolite-packed anaerobic bioreactor: Bacterial diversity and community structure shifts. Journal of Environmental Management. 279: 111558.

Pang Y, Zhao C, Li Y, et al. (2022) Cadmium adsorption performance and mechanism from aqueous solution using red mud modified with amorphous MnO_2. Sci Rep 12: 4424.

Park HJ, Jeong SW, Yang JK, Kim BG, Lee SM (2007) Removal of heavy metals using waste eggshell. J Environ Sci (China) 19(12): 1436-41.

Patra A, Dutta A, Mohapatra KK, Pradhan S (2020) Nickel the ultra-micronutrient: significant for plant growth and metabolism, Food Chem. Toxicol. 1: 35-37.

Rajic N, Stojakovic D. Jovanovic M, Logar NZ, Mazaj M, Kaucic V (2010) Removal of nickel(II) ions from aqueous solutions using the natural clinoptilolite and preparation of nano-NiO on the exhausted clinoptilolite. Applied Surface Science 257(5): 1524–1532.

Sahmoune MN (2019) Evaluation of thermodynamic parameters for adsorption of heavy metals by green adsorbents. Environmental Chemistry Letters 17: 697–704.

Segneanu AE, Marin CN, Vlase G, et al. (2022) Highly efficient engineered waste eggshell-fly ash for cadmium removal from aqueous solution. Sci Rep. 12: 9676.

Sharma AK, Desnavi S, Dixit C, Varshney U, Sharma A (2014) Extraction of nickel nanoparticles from electroplating waste &their application in production of bio-diesel from biowaste, International Journal of Chemical Engineering and Applications 6(3).

Sinyoung S, Taweekitwanit E, Kajitvichyanukul P (2015) Effects of Nickel on properties of cement mortar derived from the co-burning of industrial waste and its leaching behavior, Adv.Mat.Res. 1103:121-127.
Stevens M, Batlokwa B (2017) Removal of nickel (II) and cobalt (II) from wastewater using vinegar-treated eggshell waste biomass. Journal of Water Resource and Protection, 9: 931-944.
Qasem NAA, Mohammed RH, Lawal DU (2021) Removal of heavy metal ions from wastewater: a comprehensive and critical review. npj Clean Water 4: 36.
Qiao H, Wei Z, Yang H, Zhu L, Yan X (2009) Preparation and characterization of NiO nanoparticles by anodic arc plasma method, Journal of Nanomaterials vol. 2009, Article ID 795928, 5 pages.
Thommes M, Kaneko K, Neimark AV, Olivier JP, et. al. (2015) Physisorption of gases, with special reference to the evaluation of surface area and pore size distribution (IUPAC Technical Report). Pure and Applied Chemistry. 87(9-10).
Tripathi A, Ranjan MR (2015) Heavy metal removal from wastewater using low cost adsorbents, J Bioremed Biodeg. 6: 315.
Tsai WT, Yang JM, Hsu HC, Lin CM, Lin KY, Chiu CH (2008) Development and characterization of mesoporosity in eggshell ground by planetary ball milling. Microporous and Mesoporous Materials 111(1-3): 379–386.
Vischetti C, Marini E, Casucci C, De Bernardi A (2022) Nickel in the environment: bioremediation techniques for soils with low or moderate contamination in European Union, Environments 9: 133.
Waheed M, Yousaf M, Shehzad A, Inam-Ur-Raheem M, Khan MKI et. al. (2020) Channelling eggshell waste to valuable and utilizable products: A comprehensive review. Trends in Food Science & Technology 106:78–90
Wang J, Guo X, (2020) Adsorption kinetic models: Physical meanings, applications, and solving methods. Journal of Hazardous Materials, 390: 122156.
Wang Z, Xu W, Jie F, et al. (2021) The selective adsorption performance and mechanism of multiwall magnetic carbon nanotubes for heavy metals in wastewater. Sci Rep.11:16878.
Xin Y, Li C, Liu J, Liu J, Liu Y, He W, Gao Y, (2018) Adsorption of heavy metal with modified eggshell membrane and the *in situ* synthesis of Cu-Ag/modified eggshell membrane composites. R. Soc. Open Sci. 5(9):180532.
Yokoi R, Watari T, Motoshita M (2022) Future greenhouse gas emissions from metal production: gaps and opportunities towards climate goals, Energy Environ. Sci. 15: 146.
Zendelska A, Golomeova M, Jakupi Š, Lisičkov K, Kuvendžiev S, Marinkovski M (2018) Characterization and application of clinoptilolite for removal of heavy metal ions from water resources, Geologica Macedonica 32(1): 21–32.
Zhai QZ, Li XD (2019) Efficient removal of cadmium (II) with SBA-15 nanoporous silica: studies on equilibrium, isotherm, kinetics and thermodynamics. Appl Water Sci. 9: 143.

Acknowledgments:
The "Coriolan Drăgulescu" Institute of Chemistry of Romanian Academy is acknowledged for providing access to its facilities for BET measurements.

Ethical Approval: No prior ethical approval was necessary for the study.

Consent to participate: No human subjects were included in the study. Consent was not required.

Consent to Publish: Not applicable

Author Contributions: Conception and design of study: Adina-Elena Segneanu, Ioan Grozescu; Methodology: Adina-Elena Segneanu; Athanasios Salifoglou; Aquisition of data: Maria Mihailescu. Cornelia Muntean, Roxana Trusca; Claudiu Cepan; Analysis and interpretation of data: Cornelia Muntean, Roxana Trusca; Daniel Herea; Athanasios Salifoglou; Writing–Original Draft Preparation: Adina-Elena Segneanu; Daniel Herea; Cornelia Muntean, Writing: Review&Editing: Adina-Elena Segneanu, Athanasios Salifoglou, Investigation: Maria Mihailescu; Supervision: Adina-Elena Segneanu, Athanasios Salifoglou. All authors read and approved the final manuscript.

Funding: The authors declare that no funds, grants, or other support were received during the preparation of this manuscript.

Competing interests: The authors have no relevant financial or non-financial interests to disclose.

Availability of data and Materials: The datasets and relevant material used and/or analyzed during the current study are available from the corresponding author on reasonable request.

Supplementary Files

This is a list of supplementary files associated with this preprint. Click to download.

- SupplementaryInformation2NIckel.doc